

Indian Ocean Coupled Variability and its Impact on Global Climate

Toshio Yamagata

**Climate Variations Research Program,
Frontier Research Center for Global Change,
JAMSTEC**

&

**Department of Earth and Planetary Science,
Graduate School of Science,
The University of Tokyo**

Introduction to IOD (Indian Ocean Dipole)

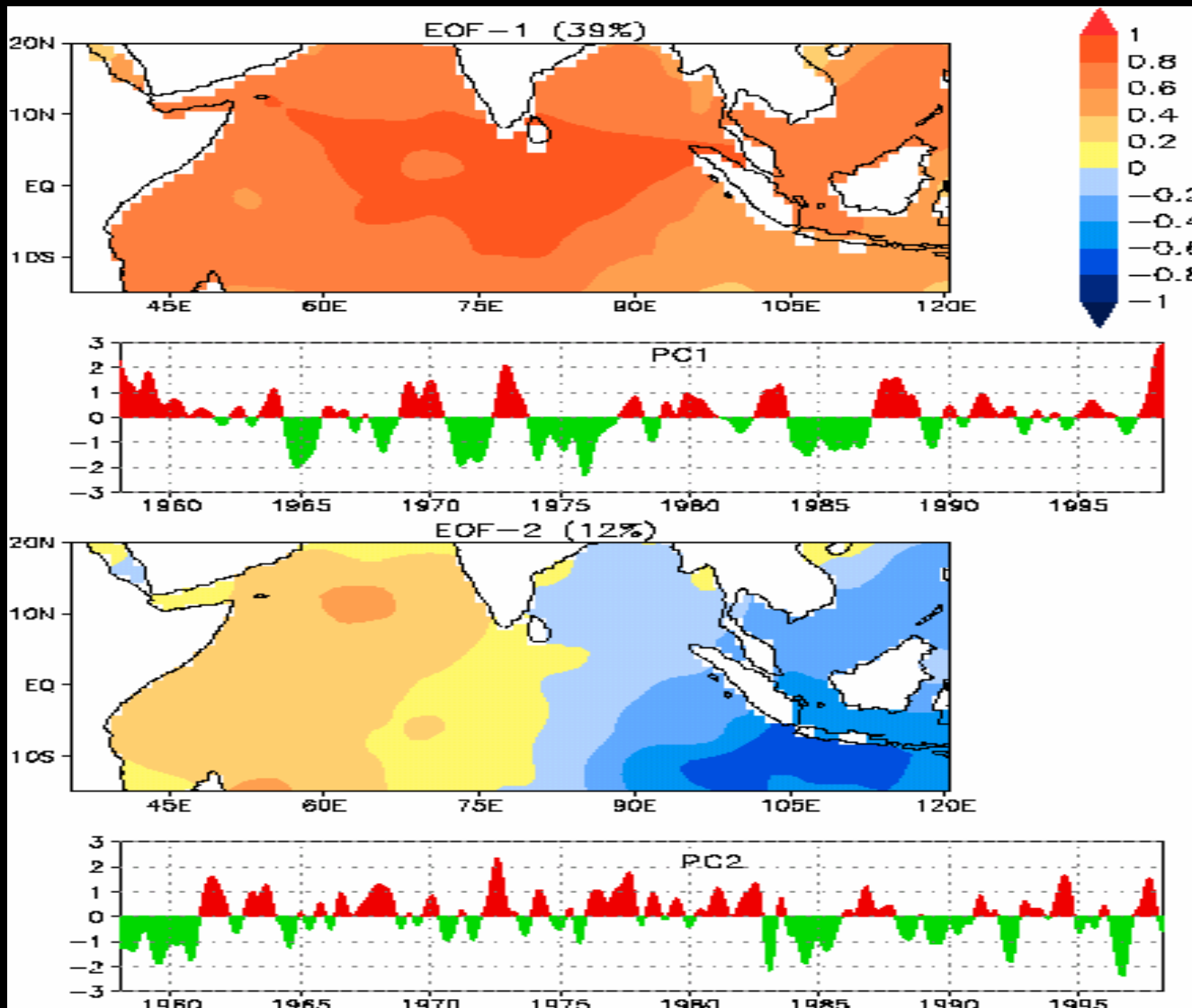
ENSO has been investigated for more than a century and is recognized as the most important manifestation of interannual climate variations of the tropical ocean–atmosphere–land coupled system.

IOD (Indian Ocean Dipole) mode was catalogued explicitly in 1999 as another important phenomenon of the tropical air–sea interaction in the Indian Ocean (cf. Saji et al., 1999; Webster et al., 1999).

Predicting as well as understanding roles of those elementary modes of climate variation is becoming more and more important under recent climate warming.

EOF analysis of SST variations of the Indian Ocean

IOD signal is captured statistically as the second mode.



EOF 1 of the Indian Ocean SST shows a basin-wide monopole structure that accounts for 39 % of total variance and is closely linked to Niño3 variability.

EOF 2, which explains 12 % , corresponds basically to the Indian Ocean Dipole.

Since EOF 1 is the dominant mode, we must be careful in appreciating the IOD.

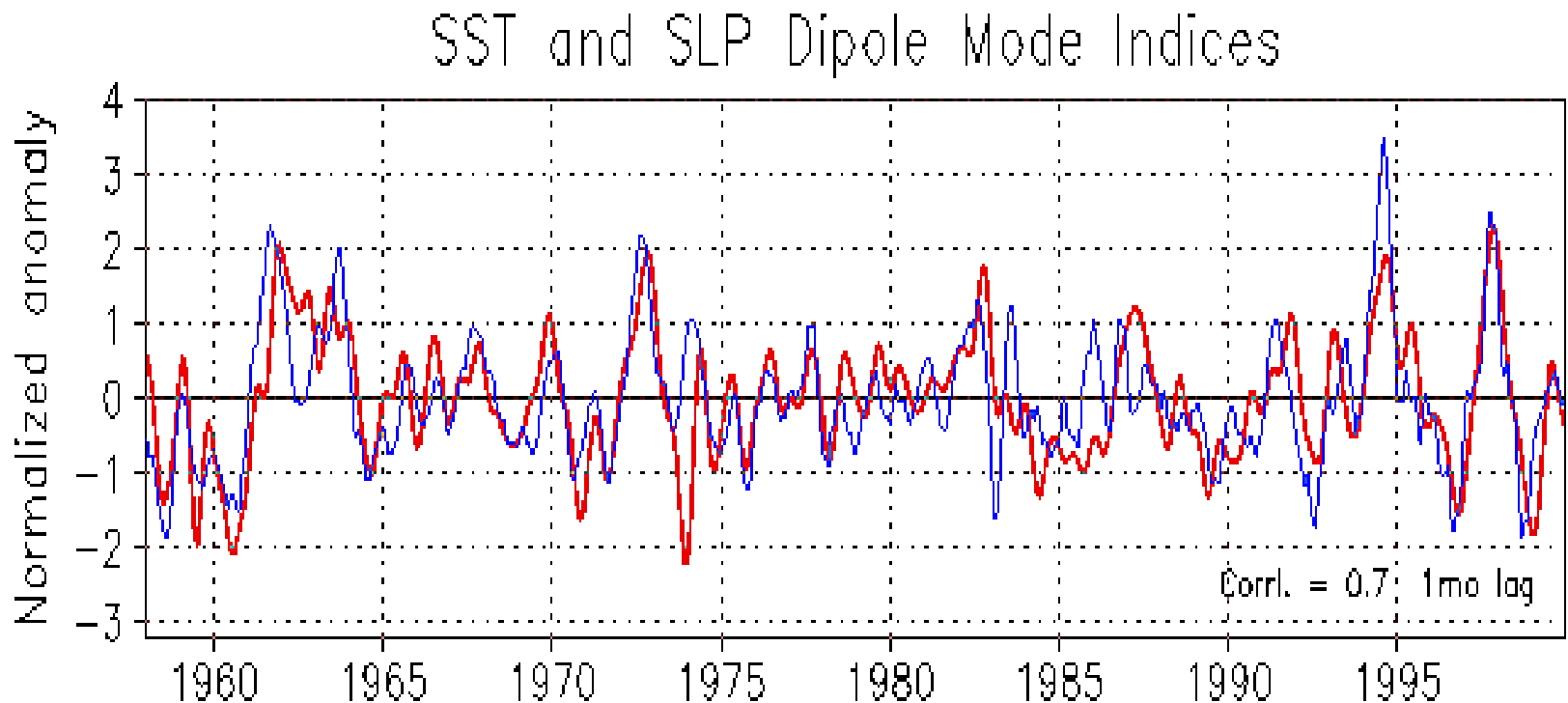
The dominance of the ENSO-related basin-wide signal, however, does not necessarily mean that the IOD always appears as the second.

The statistically lower position is due to less frequent occurrences of the IOD event compared to the ENSO event.

SST-DMI and SLP-DMI

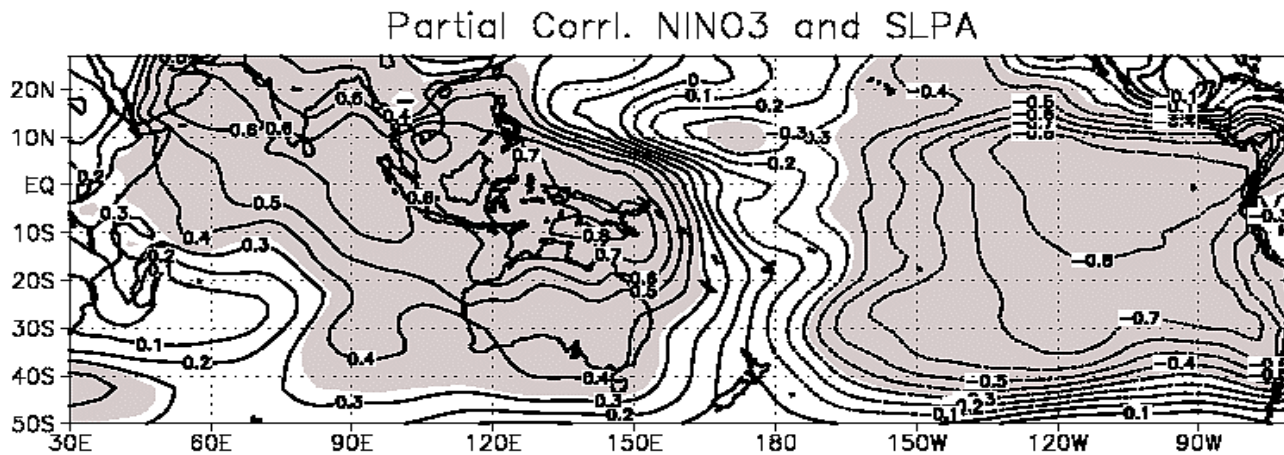
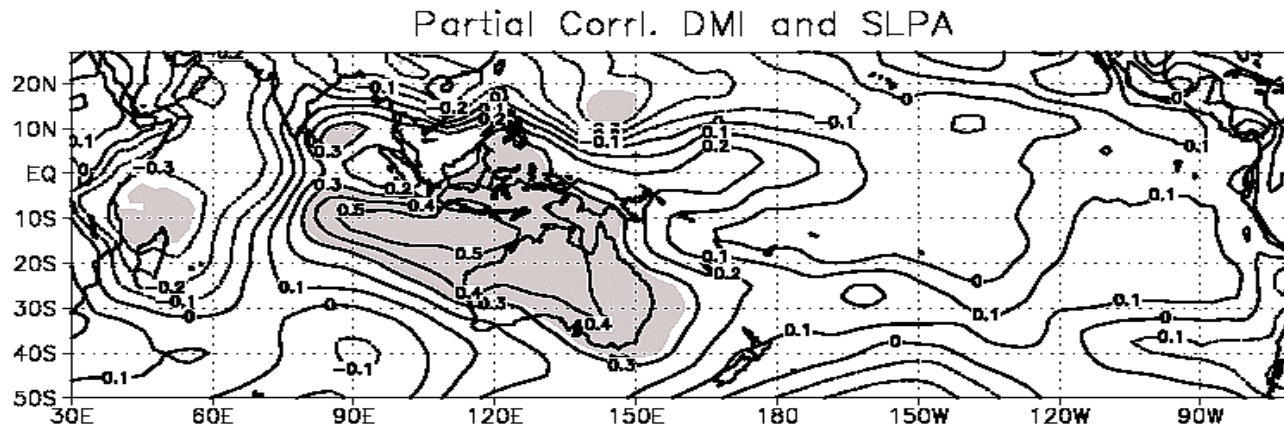
ダイポールモードの指数(双極子変動指数)

(Blue denotes SST-DMI、Red denotes SLP-DMI)



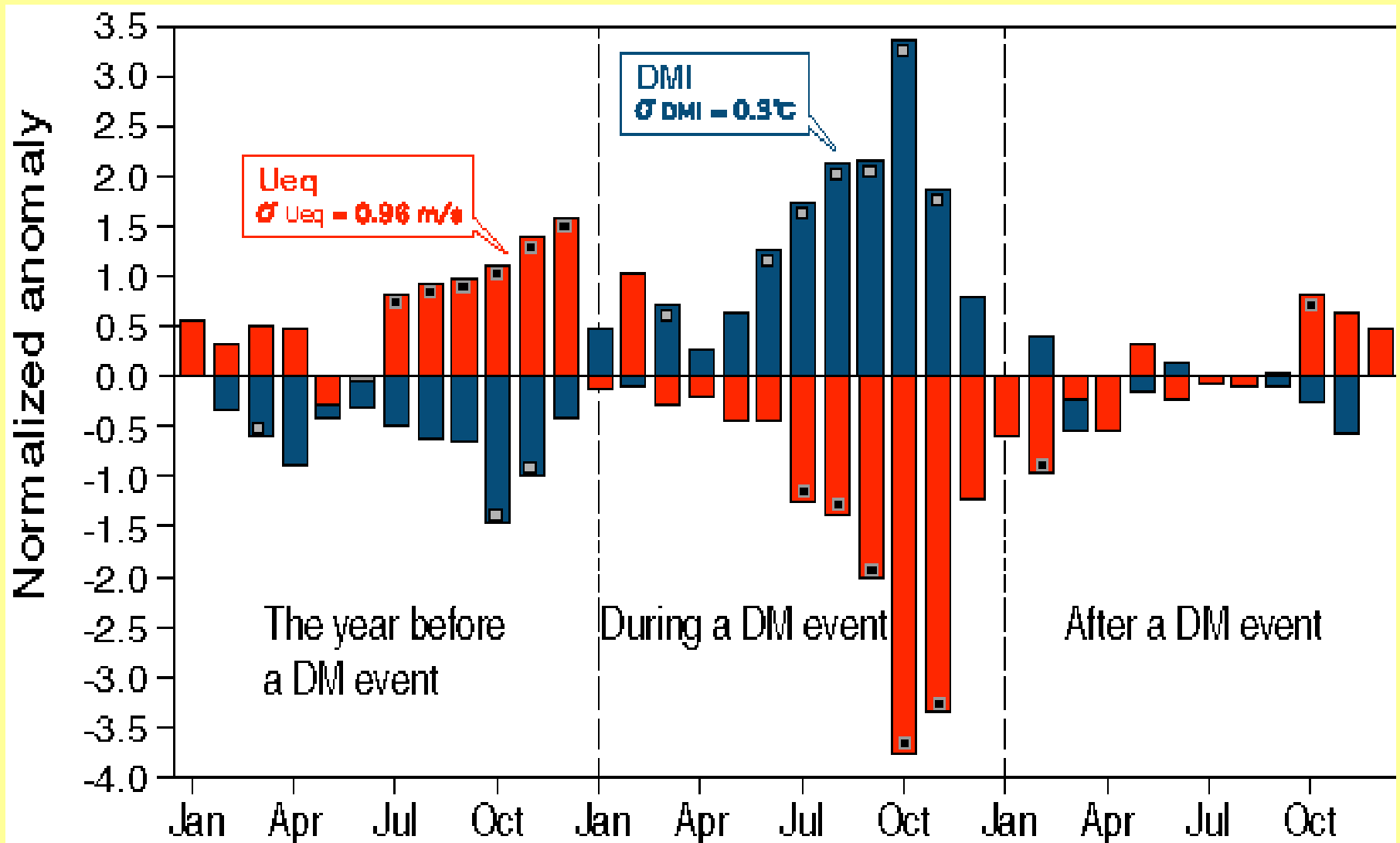
IOD Pressure Oscillation

(Behera and Yamagata, J. Met. Soc. Jpn, 81, 2003)



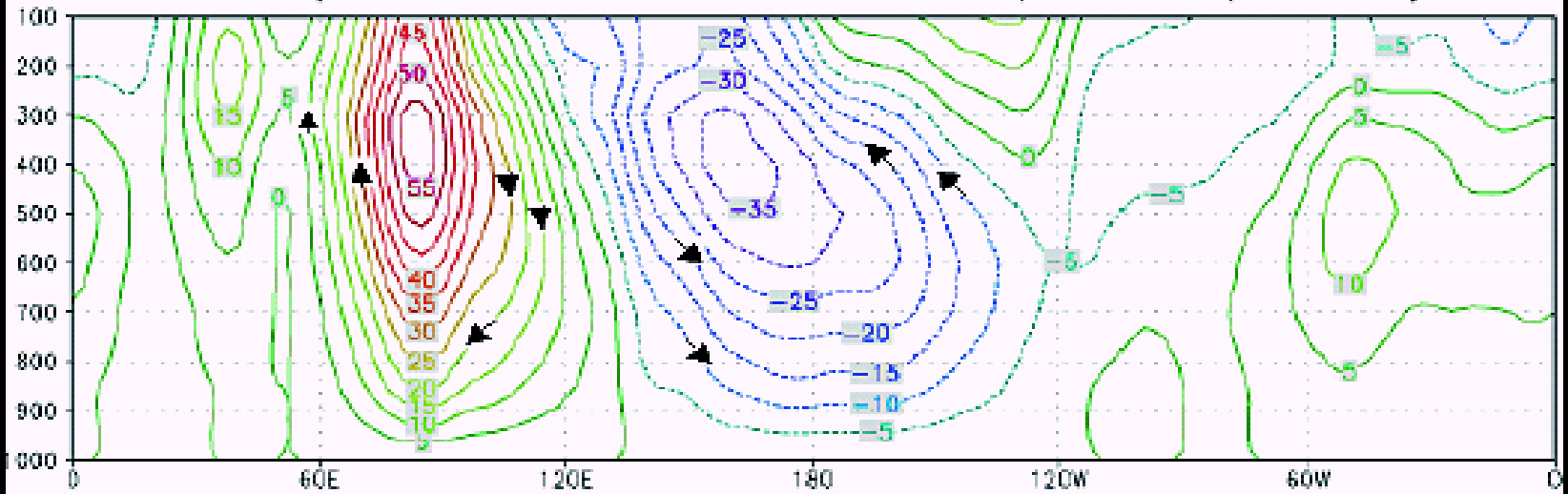
$$r_{13,2} = (r_{13} - r_{12} \cdot r_{23}) / \sqrt{(1 - r_{12}^2)} \sqrt{(1 - r_{23}^2)}$$

IOD locked to seasons

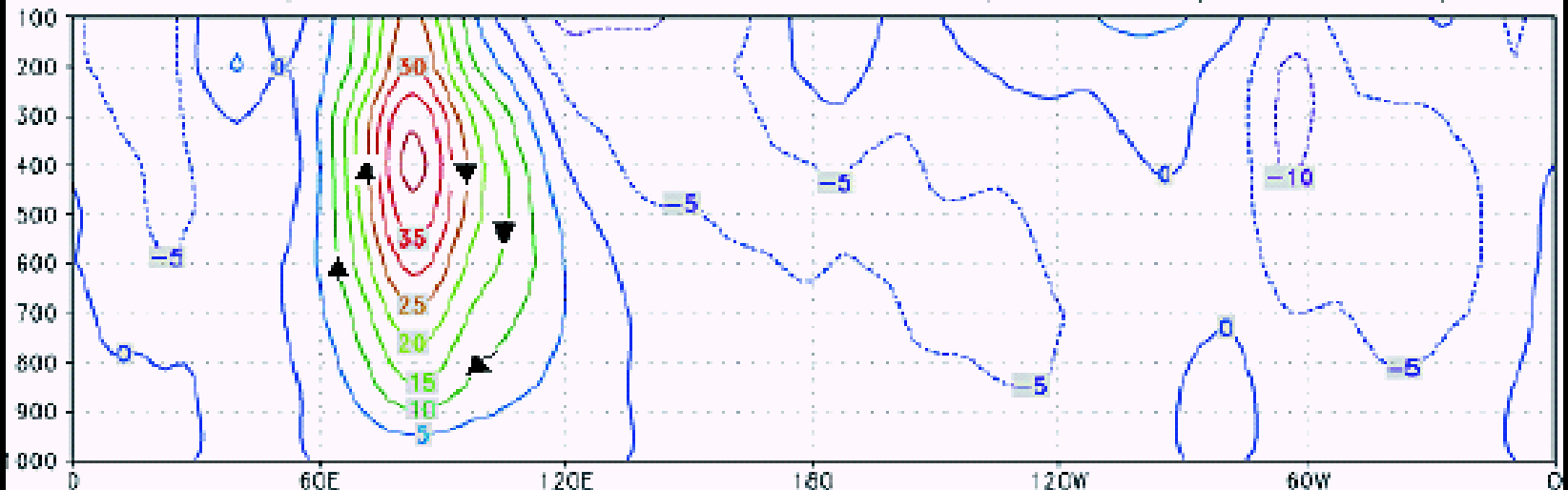


Anomalous Walker Circulation

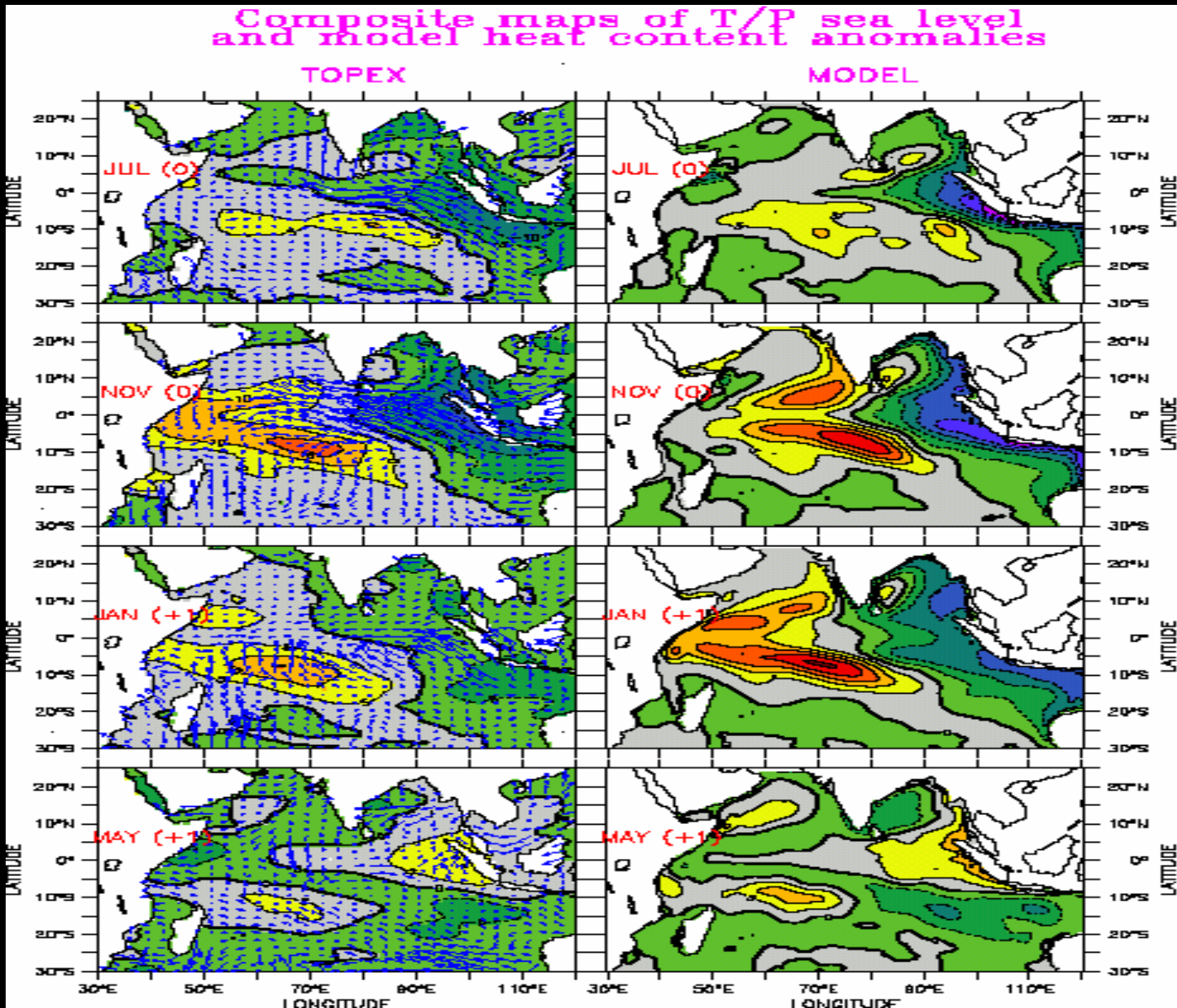
Composite Zonal Mass Flux Sep–Nov (All IOD)

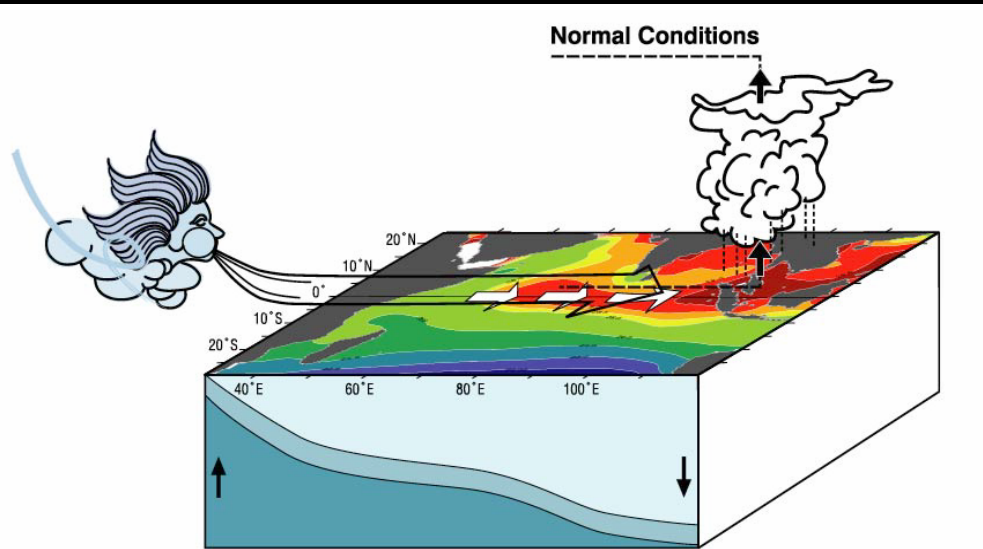


Composite Zonal Mass Flux Sep–Nov (Pure IOD)

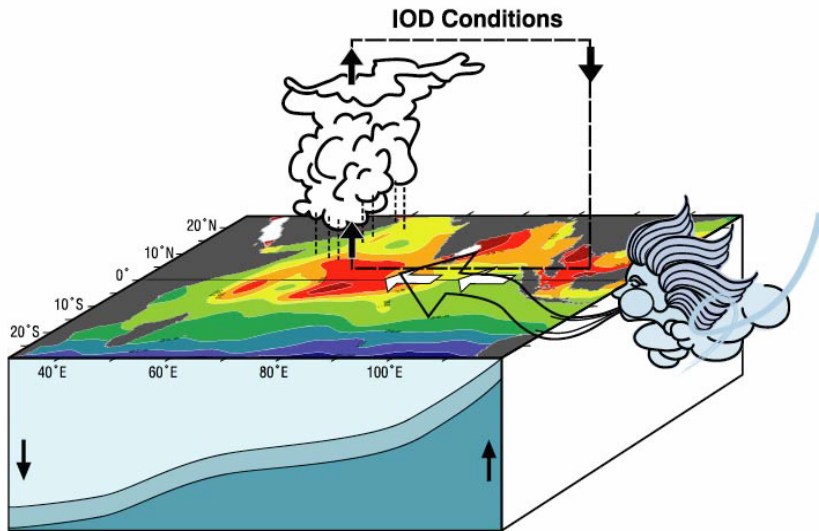


Role of ocean dynamics (Rao et al., DSR, 2002)





← Normal condition
or
Negative IOD



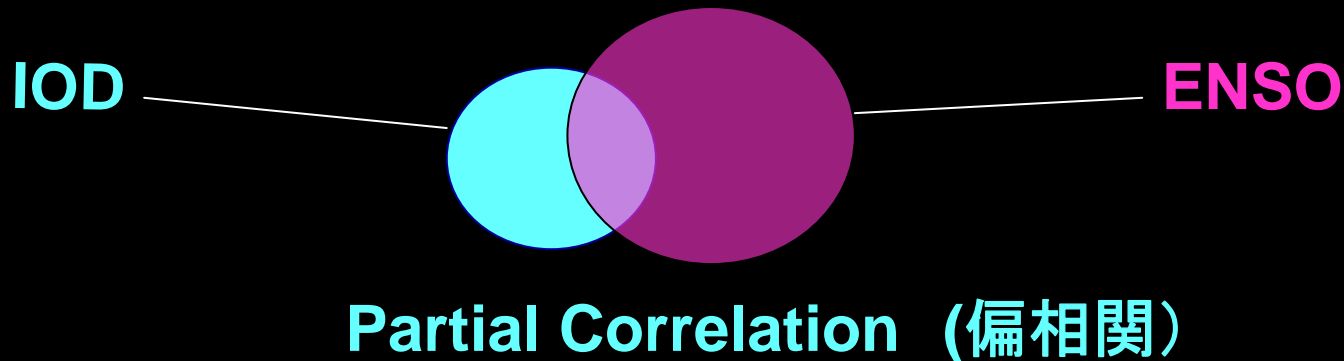
← Positive IOD

A key issue on IOD and ENSO impacts

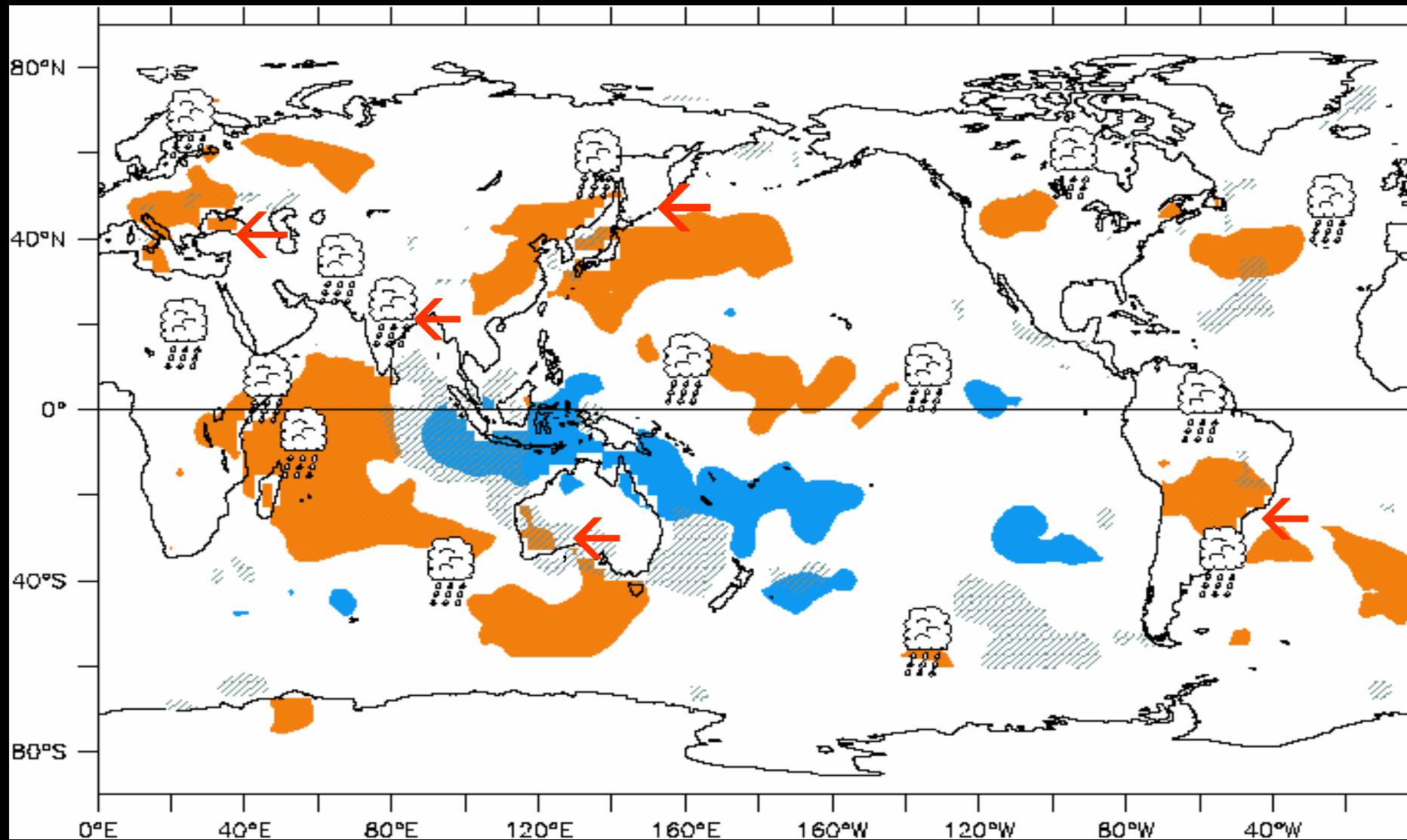
--how to appreciate the non-orthogonality of DMI and Niño3 indices--

The simultaneous correlation is 0.37; the correlation only for the season from September to November increases up to 0.54 !!

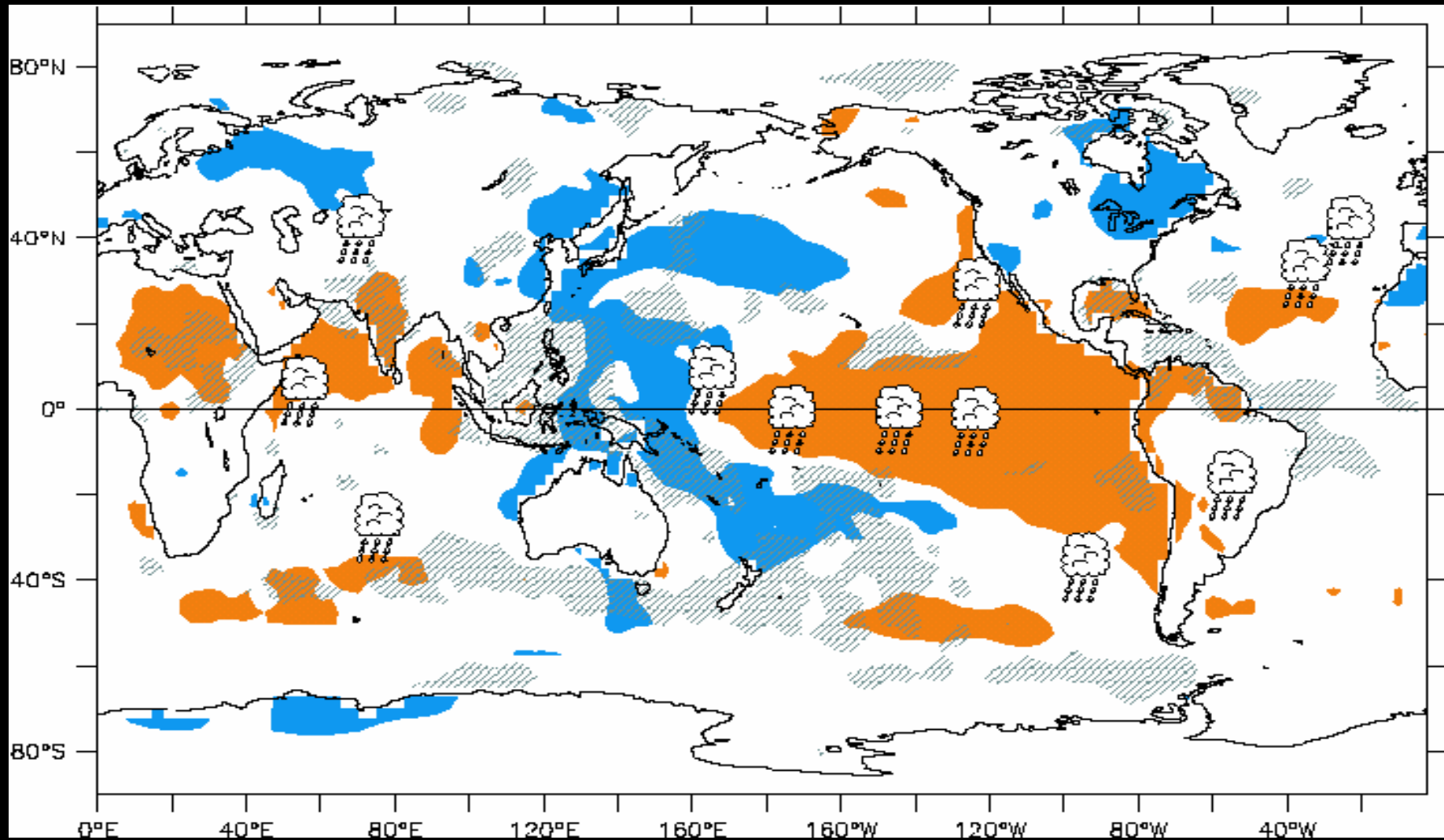
To see the real nature of respective impacts, a partial correlation analysis works



Positive IOD Influence in Boreal Summer

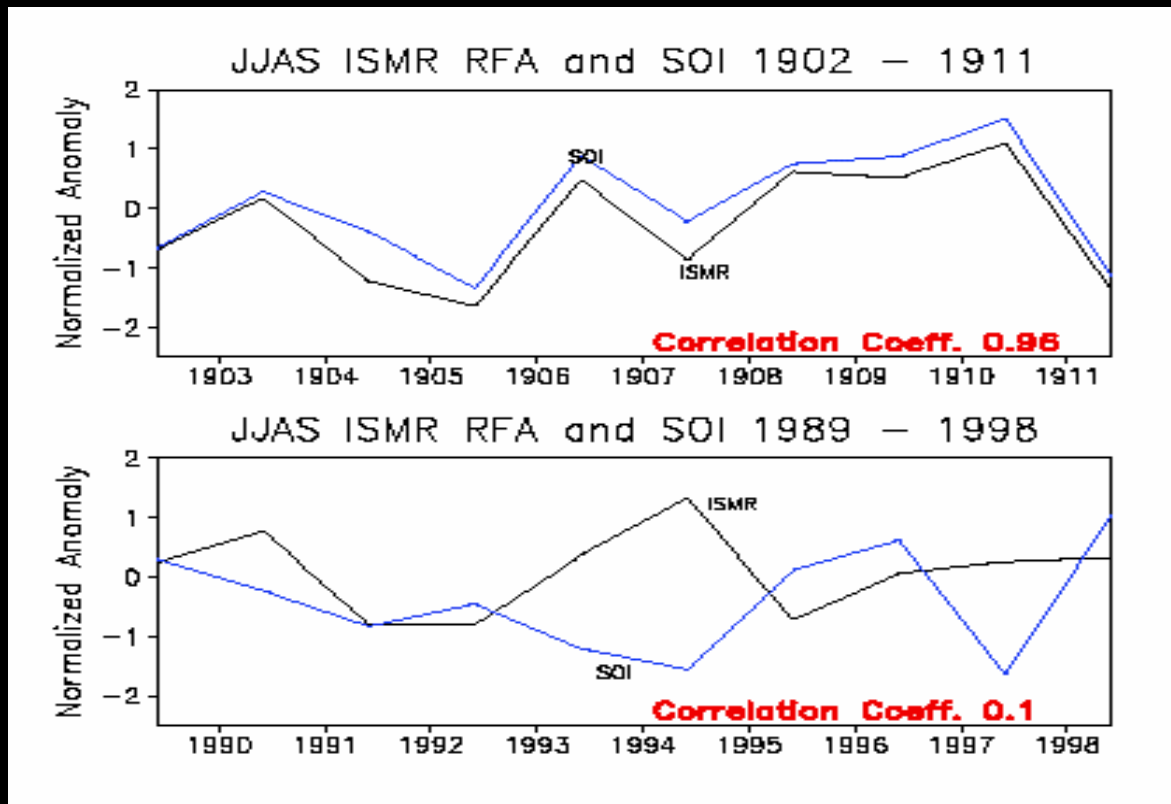


El Niño Influence in Boreal Summer



Climate evolution?!

Almost no ISMR-SOI correlation in a recent decade
in contrast to G. T. Walker's period
(Ashok, Guan and Yamagata, GRL 28,4499-4502, 2001)



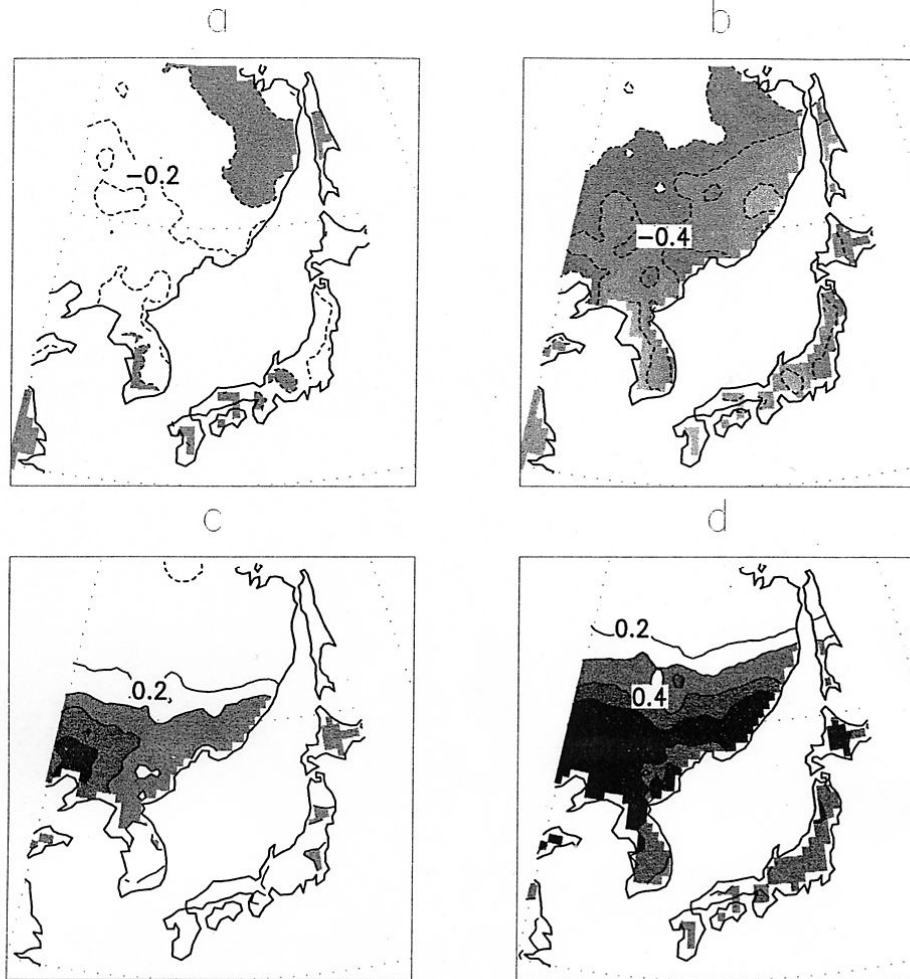
Recent increase in
positive IOD
occurrence

Each elementary climate mode does not change except for its frequency, amplitude, and phase relation with seasonal march.

Summer temperature in the Far East

Simple correlation

Partial correlation



ENSO brings
cold summer

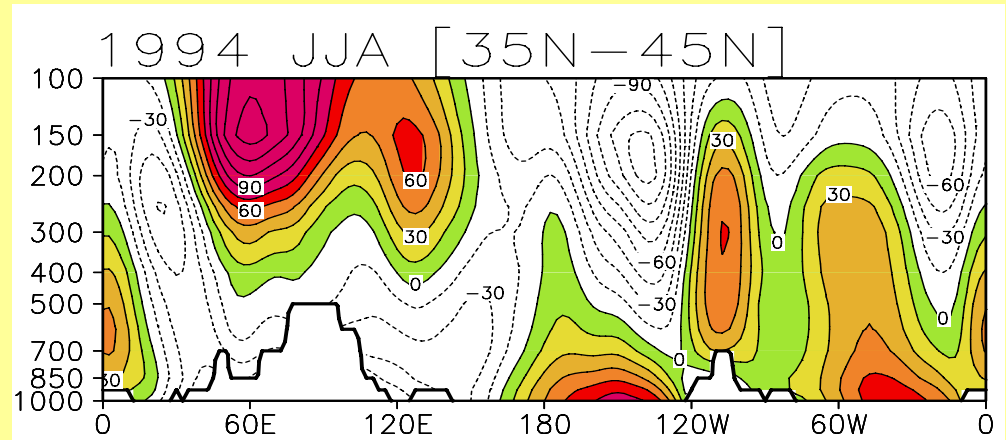
IOD brings
hot summer

Figure 7: Contribution of ENSO and IOD to the East Asian boreal summer temperatures. Simple linear correlation of a) Nino3 and c) DMI on the temperature anomaly. b) and d) represent the partial correlations of Nino3 and DMI on the temperature anomaly.

Strengthened Equivalent Barotropic Structure of Bonin High

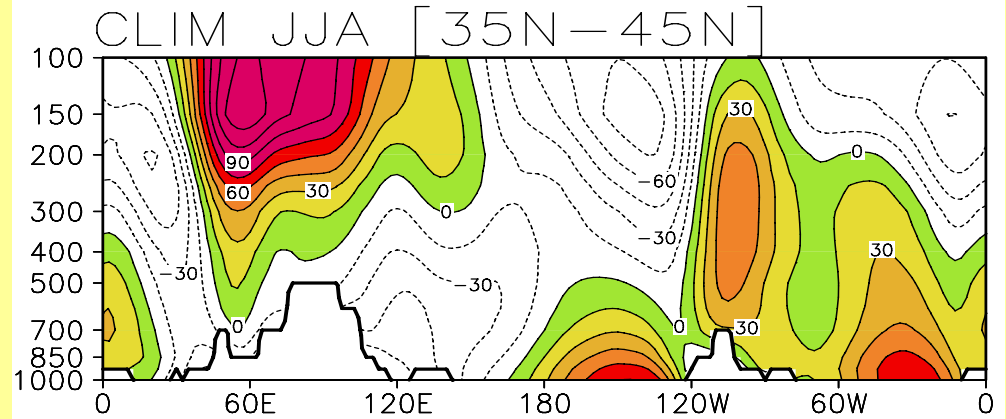
(upper)

JJA mean zonal disturbances of geopotential height averaged over [35N-45N] for 1994



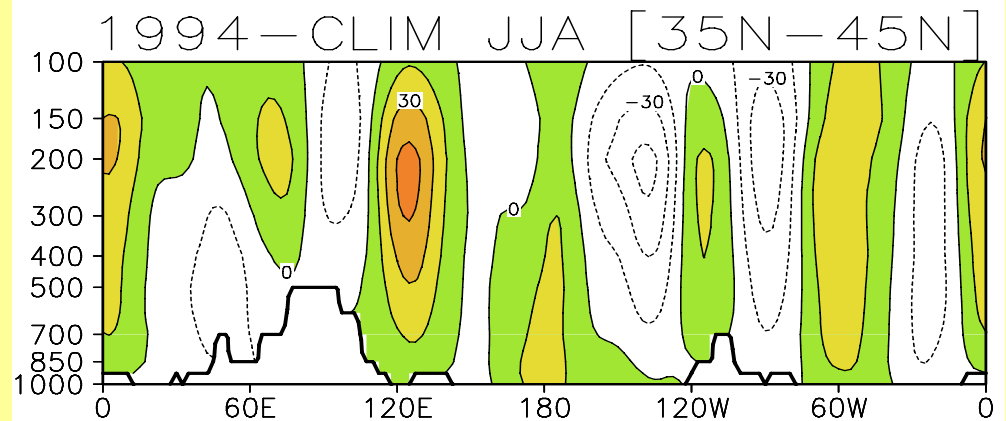
(middle)

Multi-year mean



(lower)

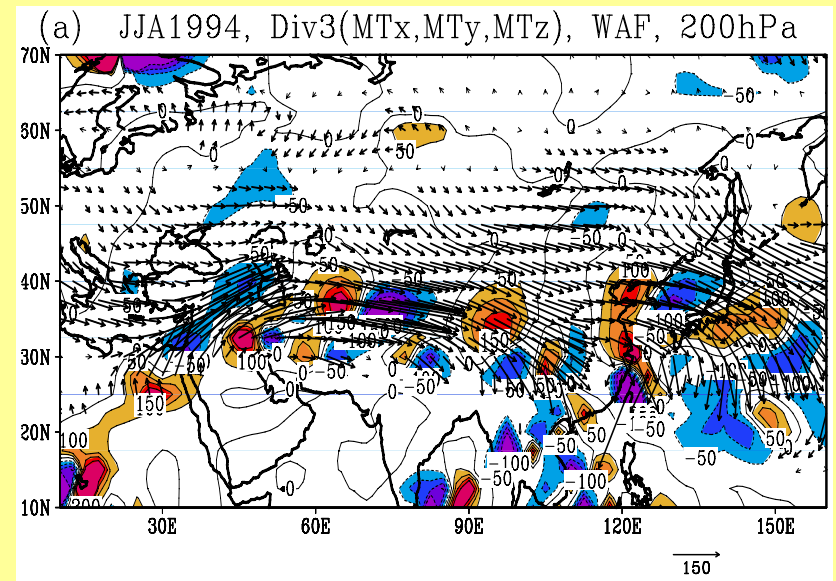
Anomalies (1994-Clim).



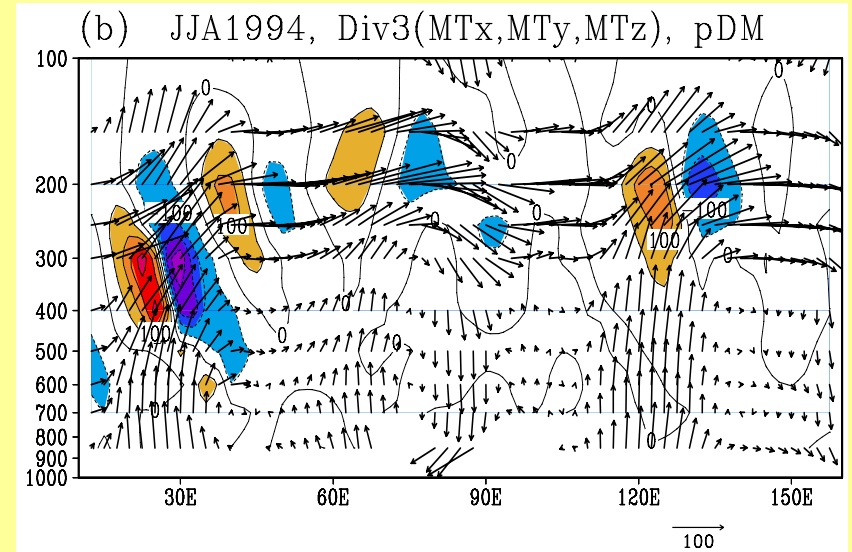
Contour intervals are 15gpm.

Wave-Activity Flux

(a) The wave-activity fluxes (in $\text{m}^2 \cdot \text{s}^{-2}$) along with the 3-dimensional divergence (to be multiplied by $1.0 \times 10^{-6} \text{ m} \cdot \text{s}^{-2}$) at 200hPa.

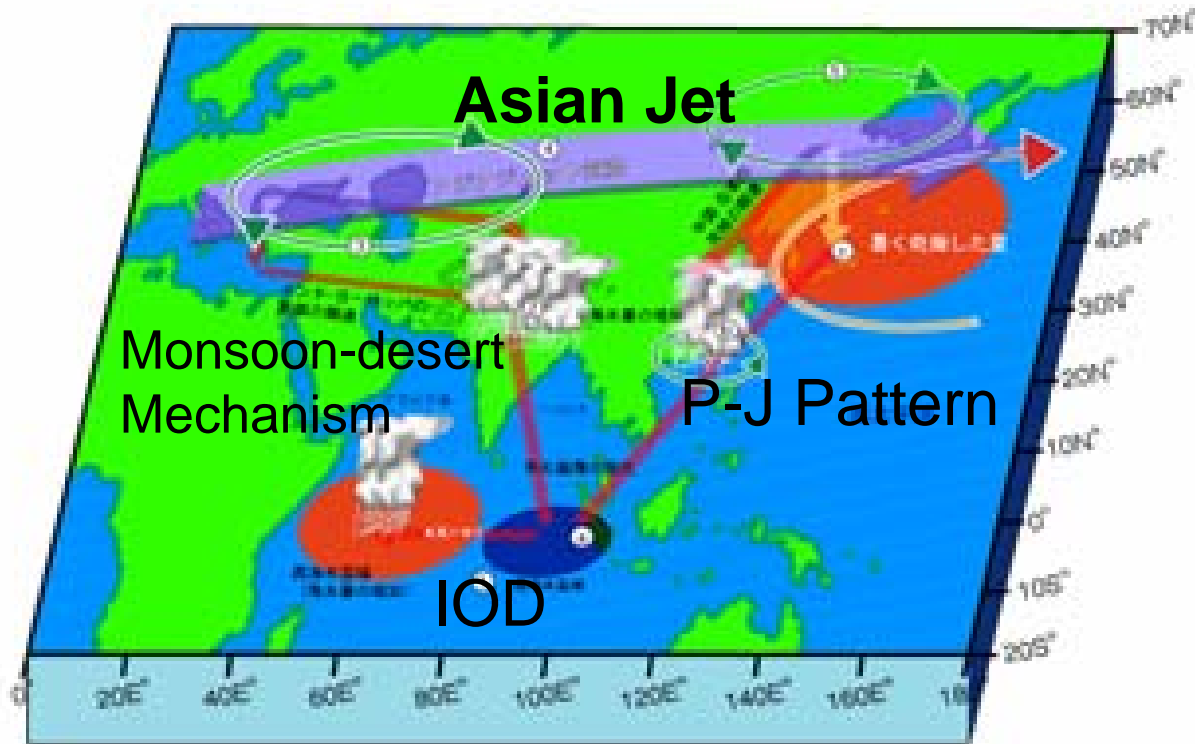


(b) The wave-activity fluxes and the 3-dimensional divergence in zonal-vertical section averaged over (35°N-45°N). The vertical component of wave-activity flux is enlarged by 10 before plotting.



ダイポールモードが遠隔地に影響するメカニズム (夏のテレコネクション)

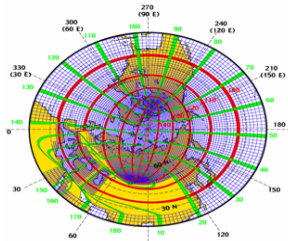
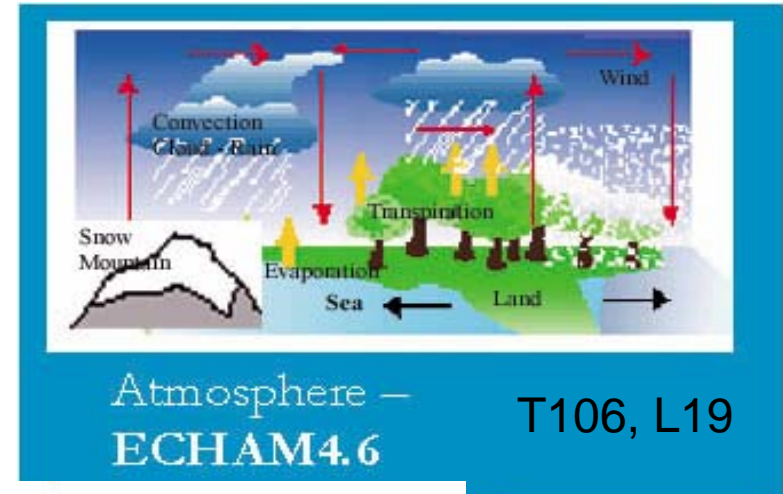
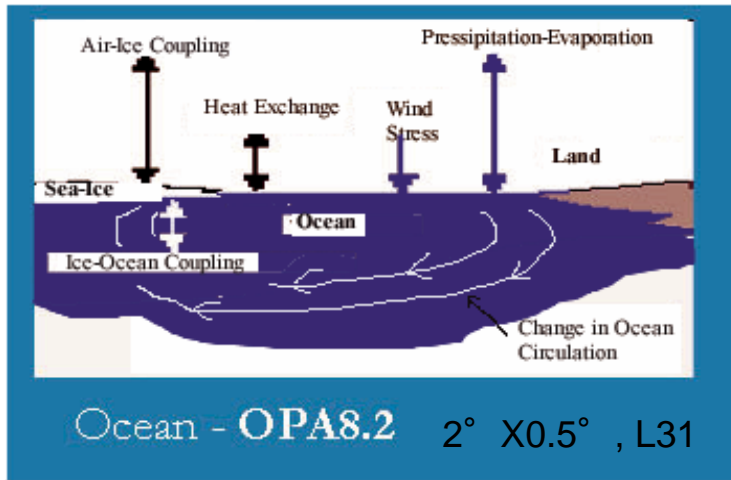
Summer Triangle Relation among IO, Mediterranean Region and Far East



インド洋ダイポールモード現象と東アジアの気候システムの「三角関係」

Simulating IOD and ENSO in a coupled GCM

Schematic view of the present version of the SINTEX-F CGCM



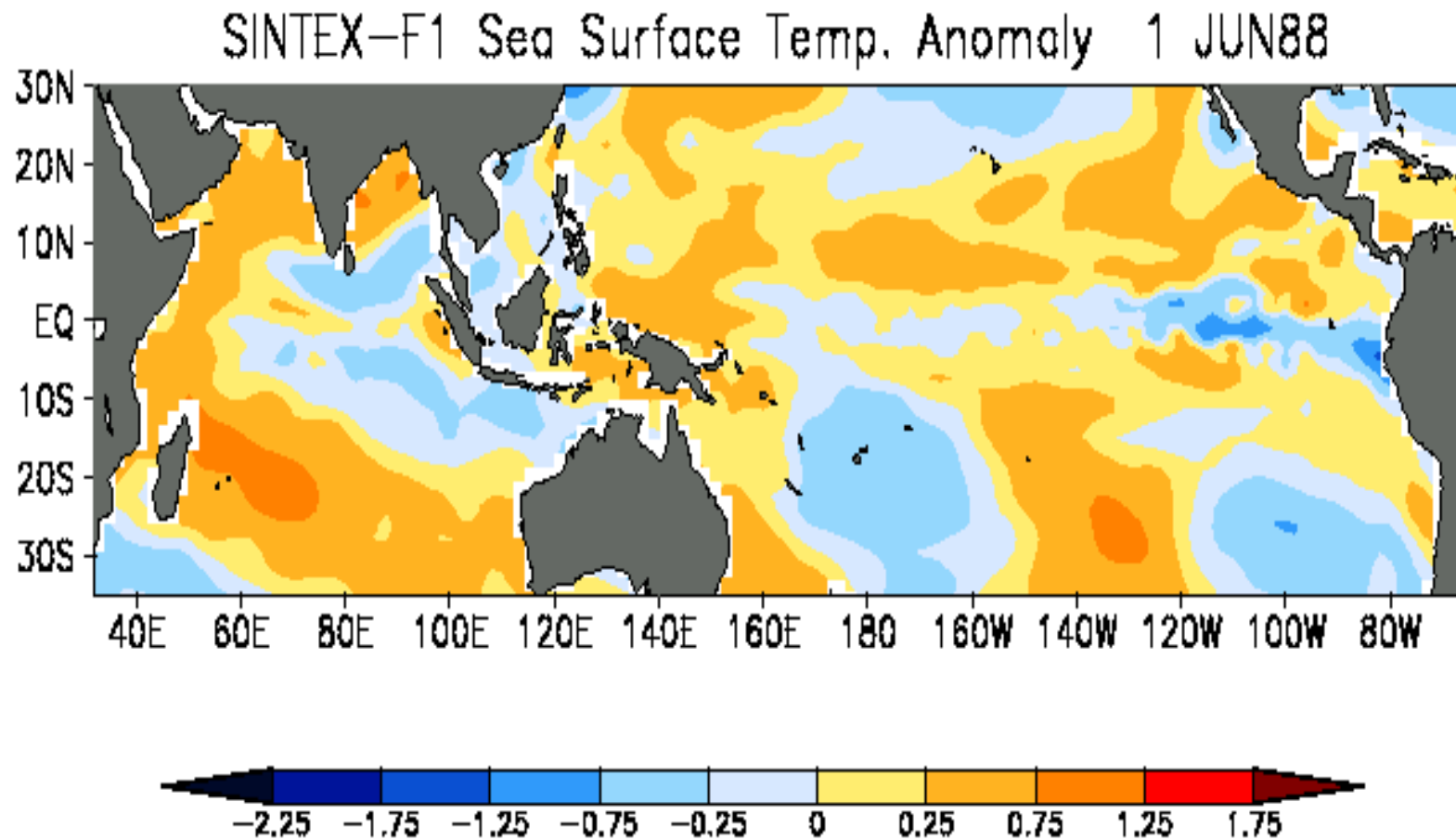
North Pole is replaced by two land points

Coupler-
OASIS4.2

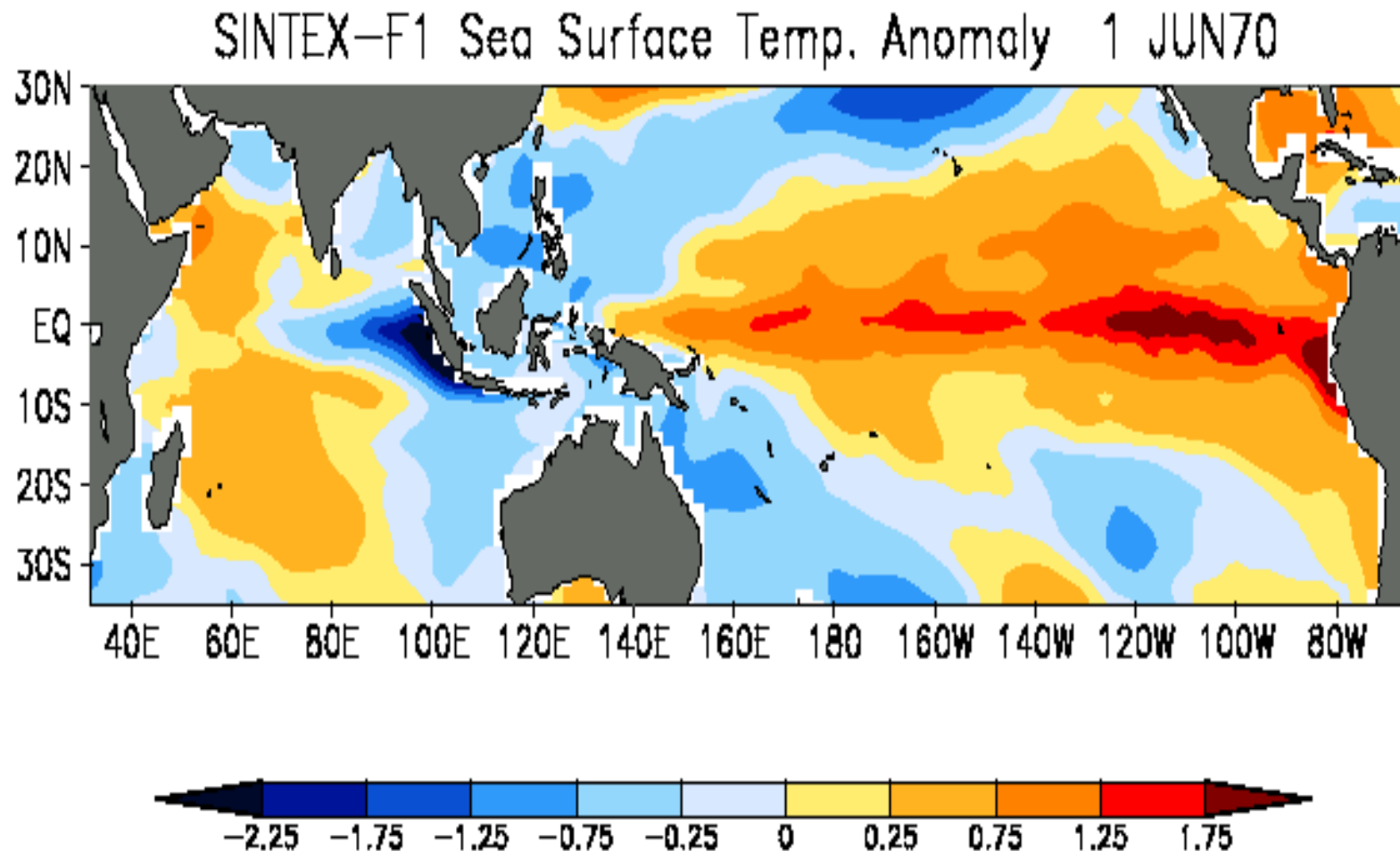
Earth Simulator



Model positive IOD during La Niña



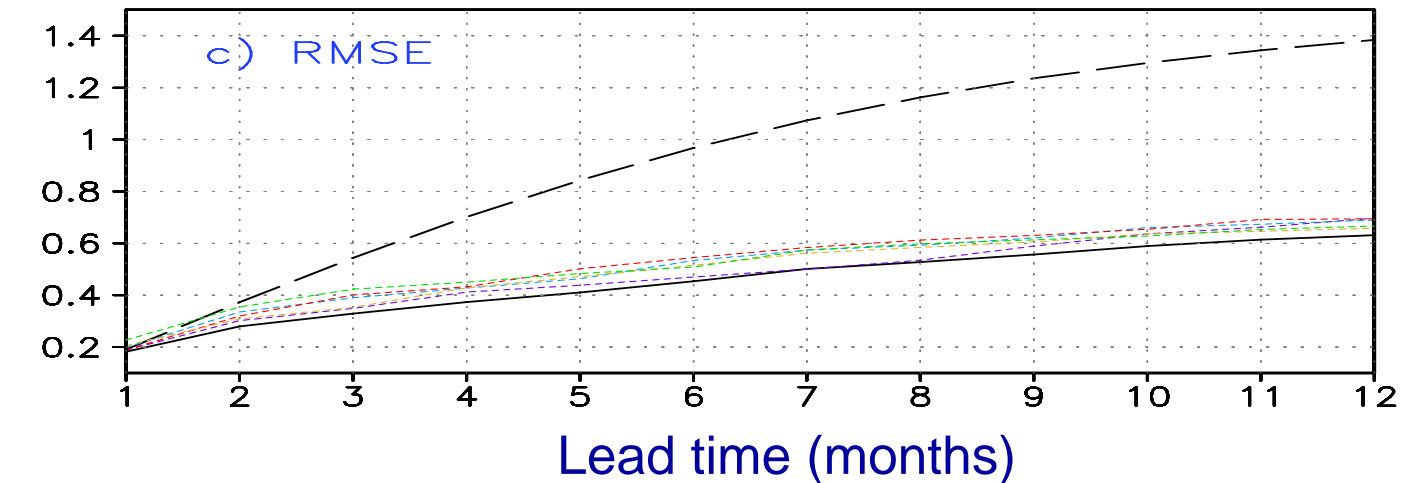
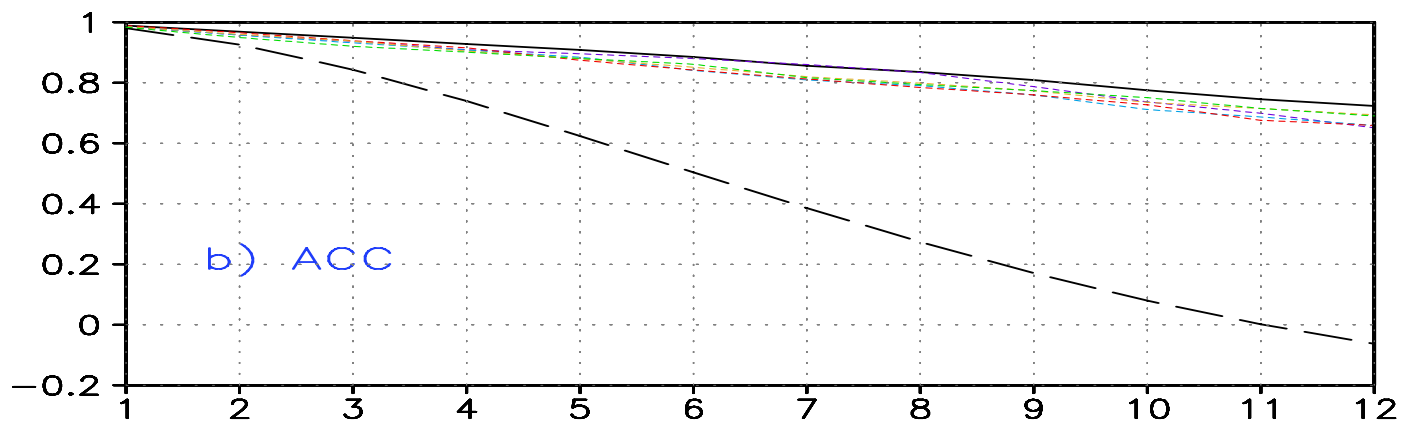
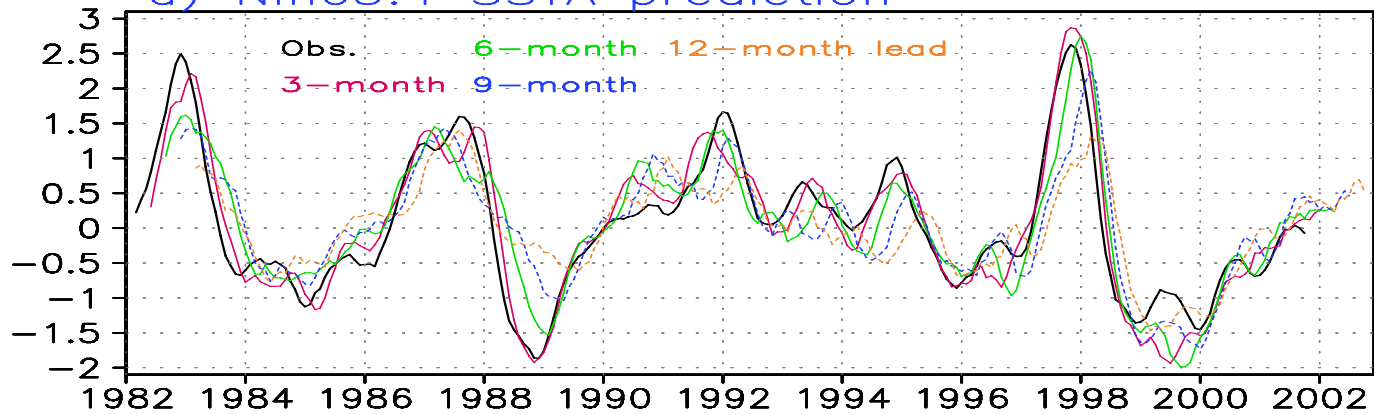
Model positive IOD during El Niño (similar to the 1997/98 event)



IOD and ENSO Statistics

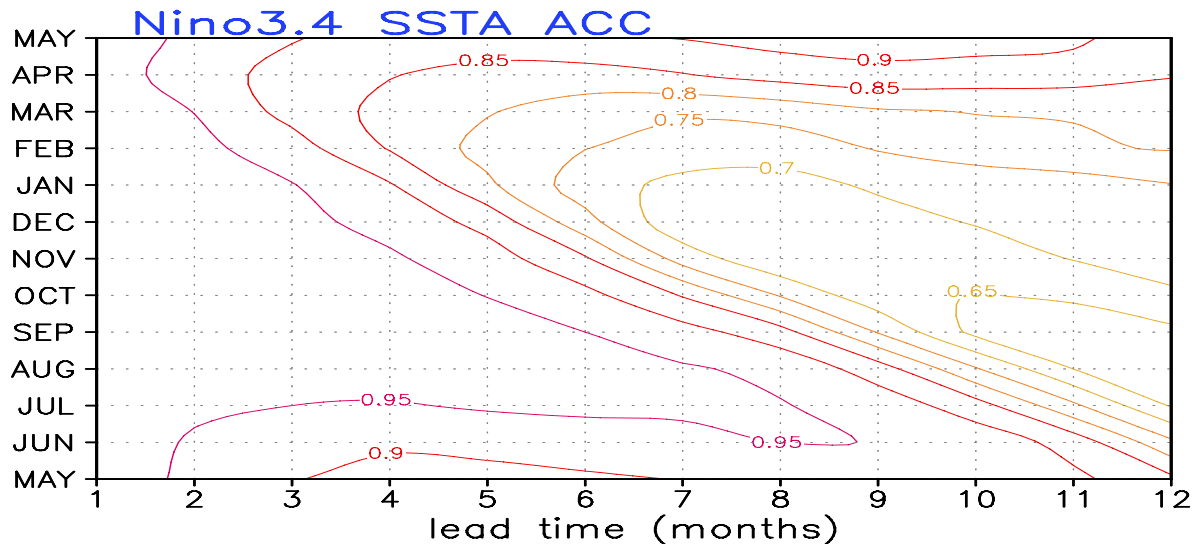
	Observed		Model	
	SD	CC	SD	CC
Indian Ocean Dipole Index	0.33	0.34 (0.54 in Sep-Nov)	0.5	0.4 (0.51 in Sep-Nov)
Niño-3	0.9		0.82	

a) Nino3.4 SSTA prediction

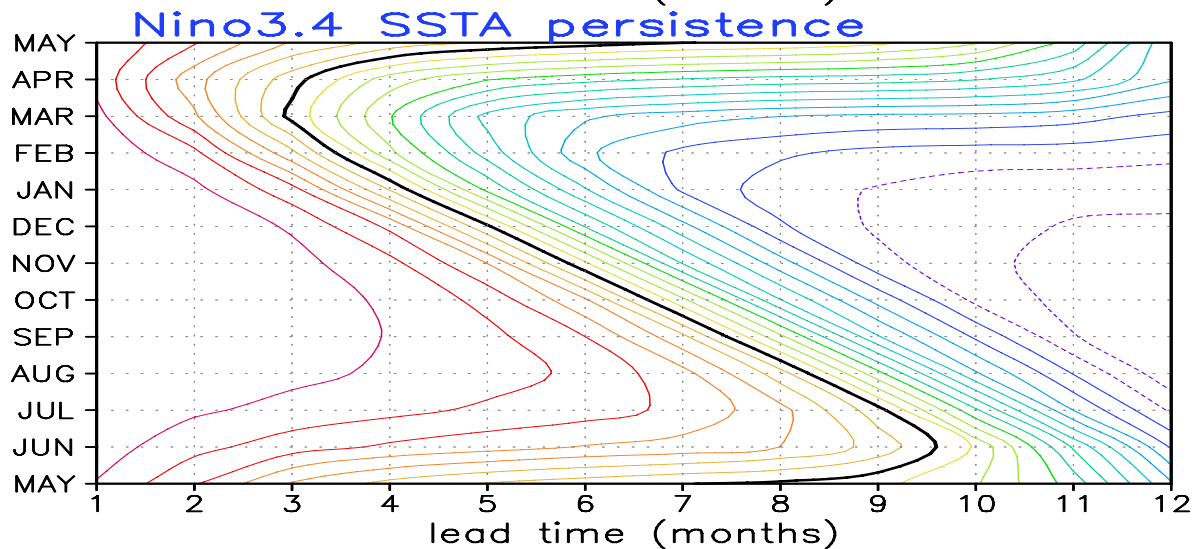


Seasonal prediction skill of ENSO (170-120W, 5S-5N)

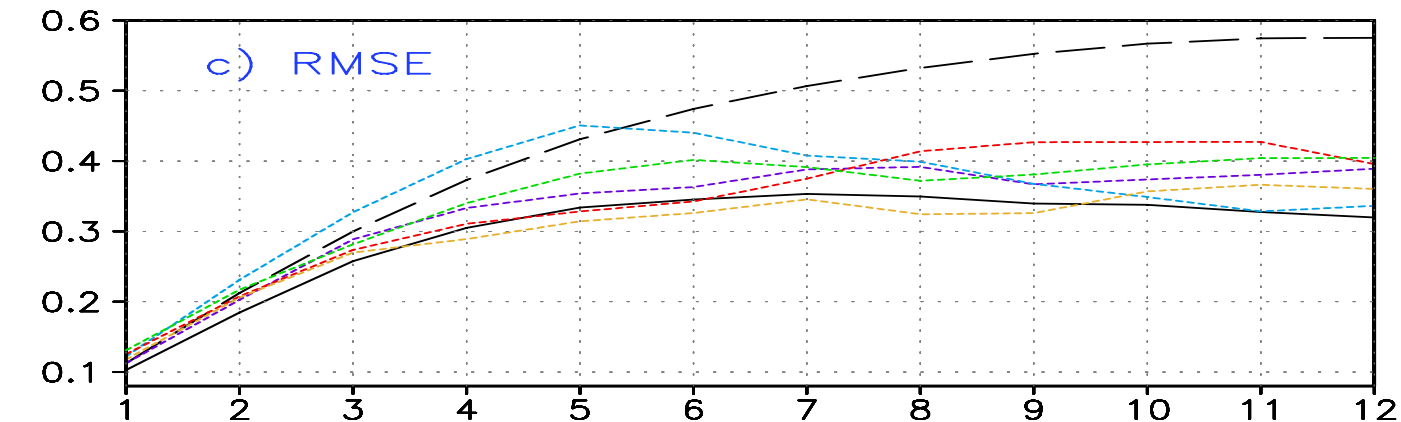
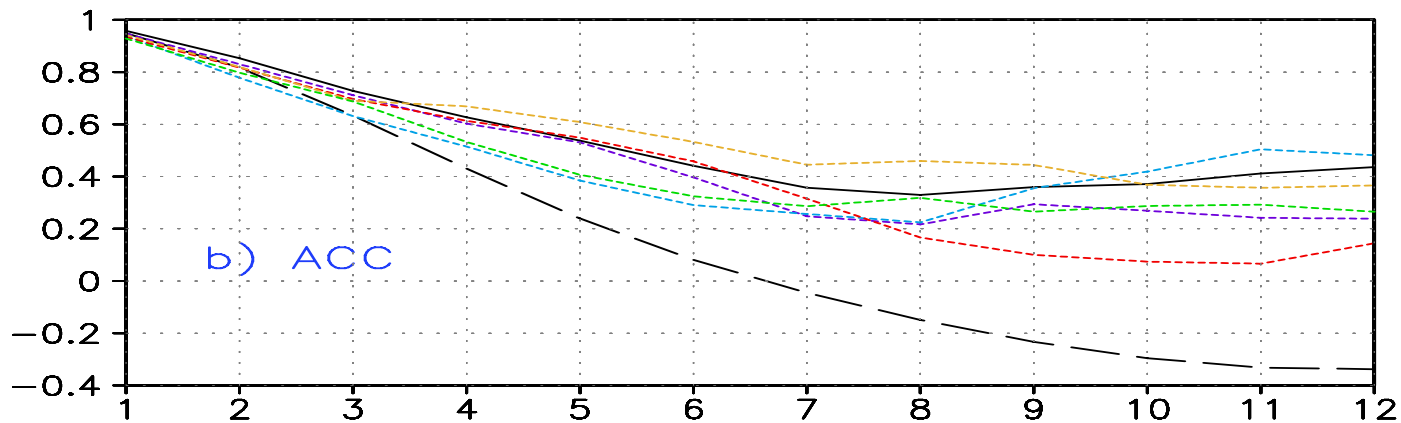
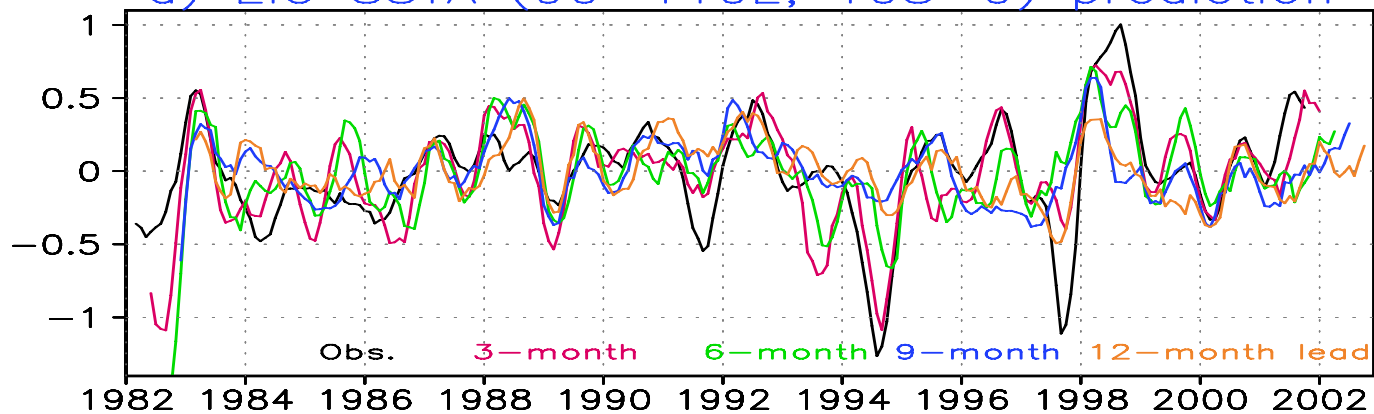
Clear Spring barrier.



Based on:
5 members
(1982-2001)



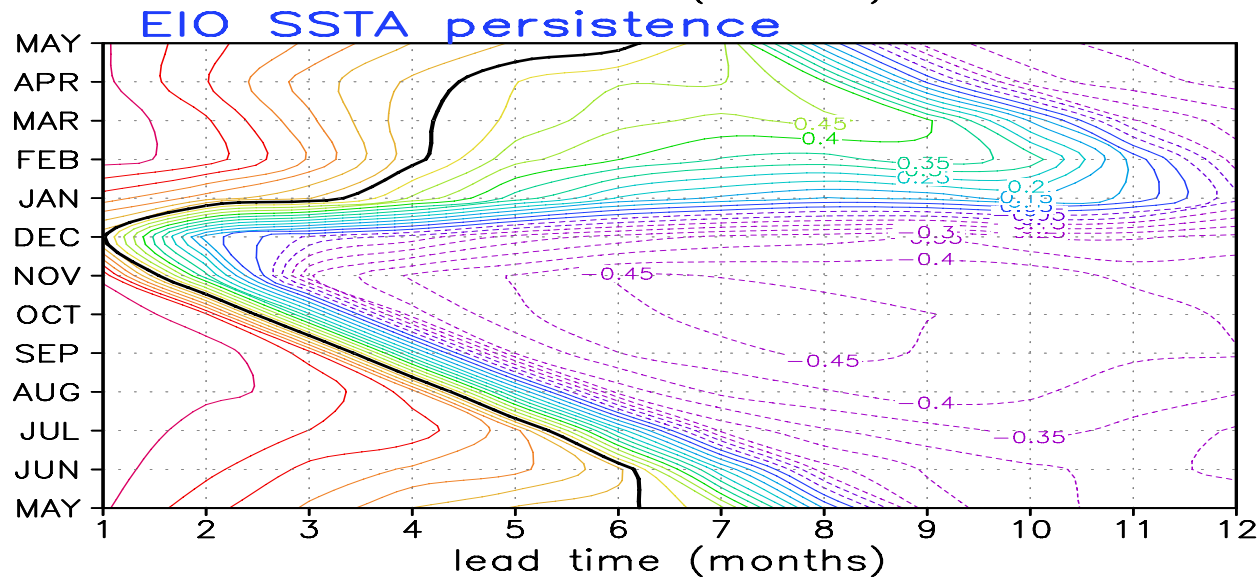
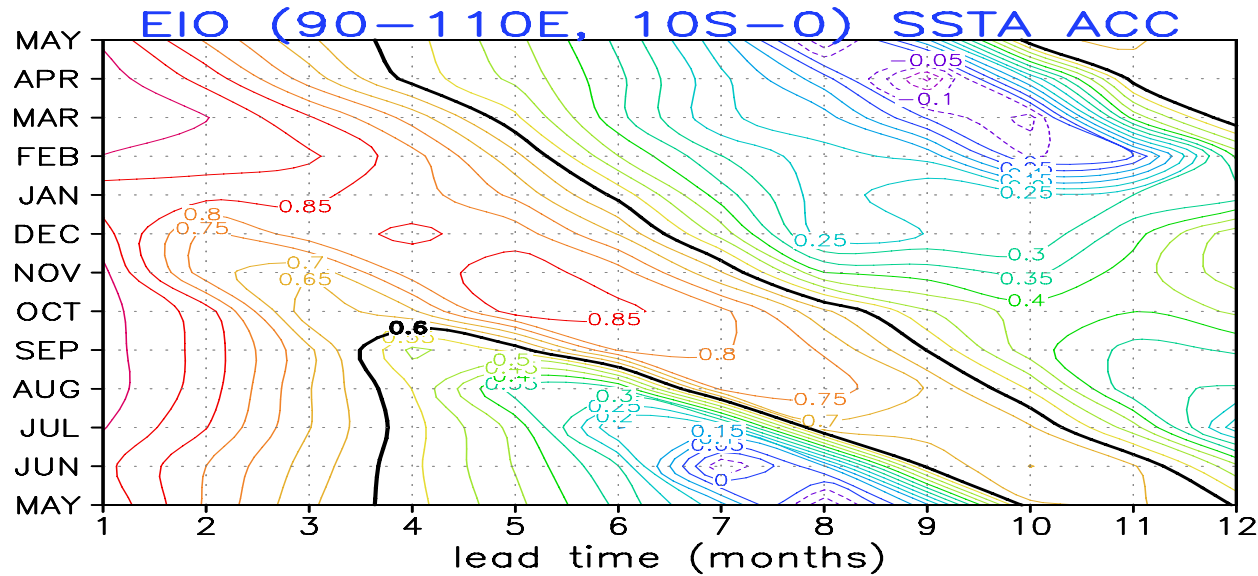
a) EIO SSTA (90–110E, 10S–0) prediction



Seasonal prediction skill of IOD (90-100E, 10S-0)

December Barrier corresponding to demise of IOD

Based on:
5 members
(1982-2001)

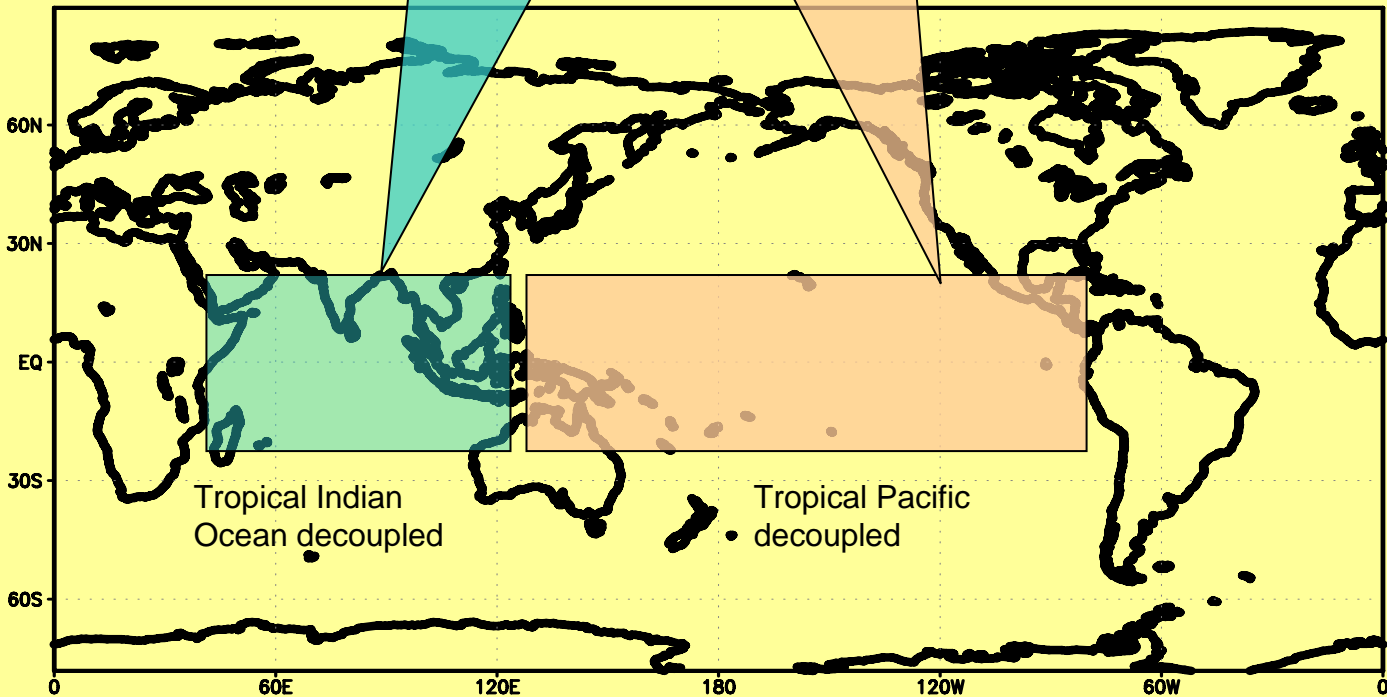


IOD vs. ENSO experiments using the SINTEX-F

CTRL Experiment 220-yr ==> SST Climatology

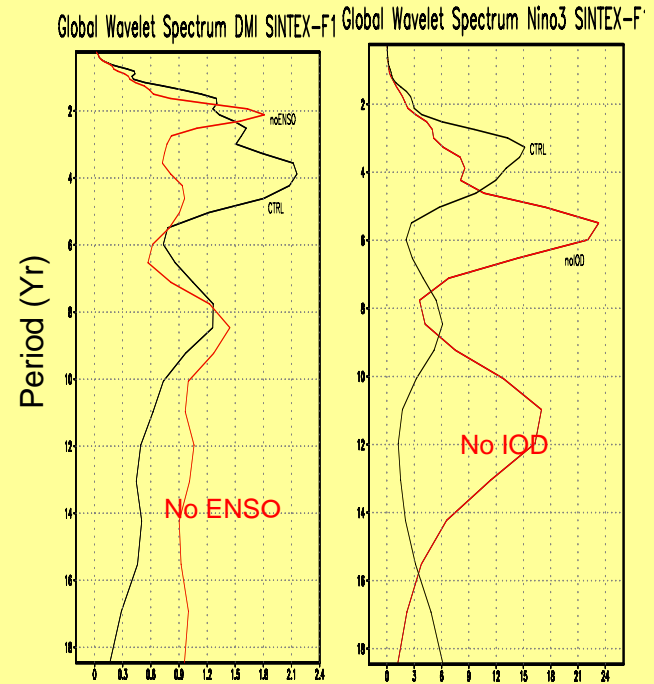
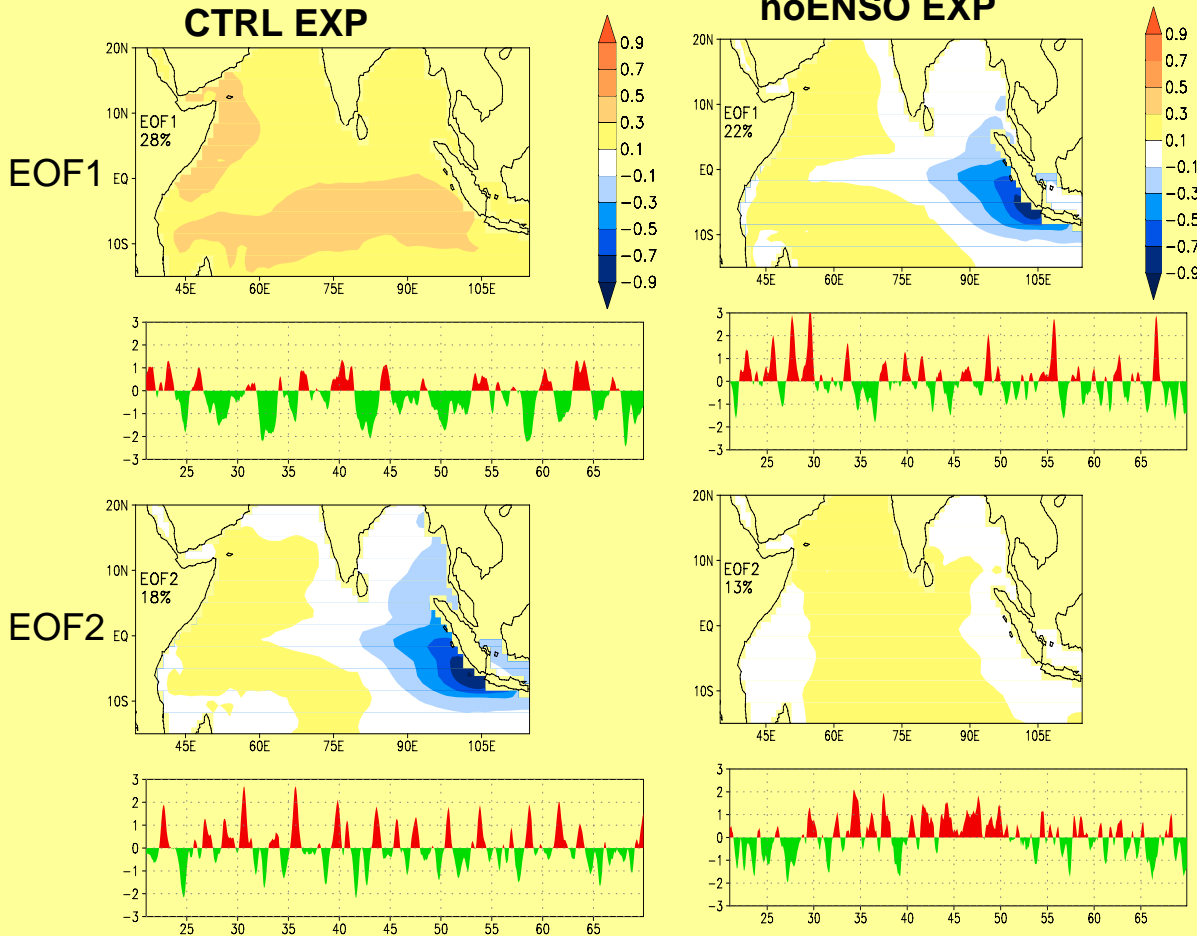
No IOD Experiment
70-yr: climatological
tropical IO SST

No ENSO Experiment
70-yr: climatological
tropical PO SST



EOF Analysis

Wavelet Power Spectrum



In the absence of ENSO, the Dipole Mode becomes the first dominant mode in the EOF analysis.

In the noENSO experiment IOD oscillations show strong biennial periodicity, whereas ENSO oscillation loses the biennial periodicity in noIOD experiment.

Summary

The Indian Ocean Dipole is a physical coupled mode in the Indian Ocean.

The IOD has the vast impact that either enhances or cancels the ENSO influences.

More serious attempts to predict IOD are necessary to meet societal needs.

Those will also contribute to enhancing ENSO prediction.

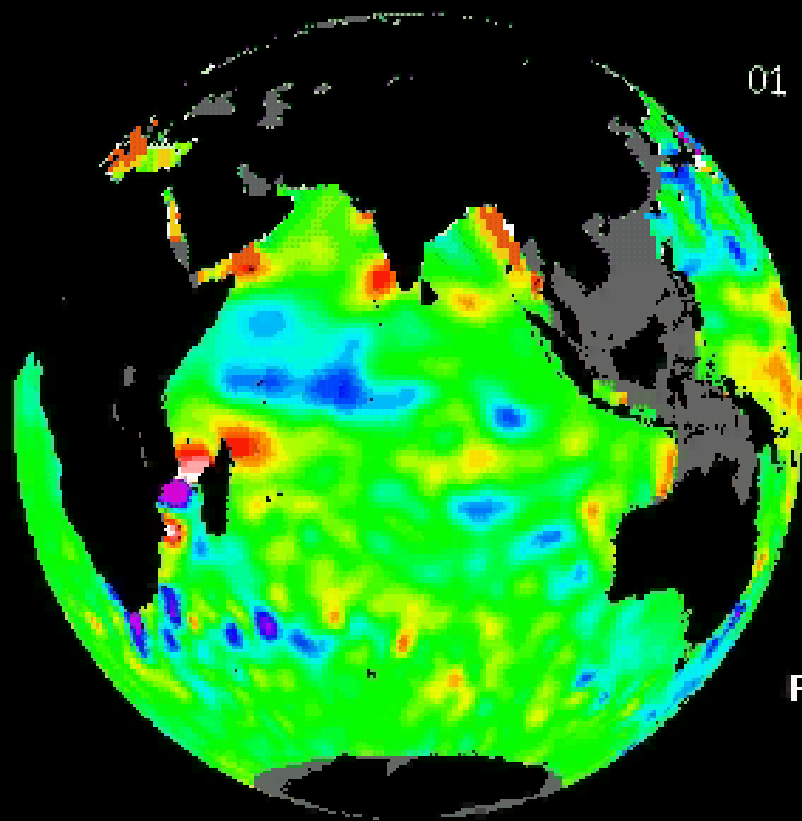
Directions

- 1) Establish a closer link between the IO observational program and EOS/GEOSS
- 2) Study inter-scale and inter-basin interactions (diurnal, ISO, semiannual, seasonal, interannual, decadal; Pacific Ocean, Atlantic Ocean, Southern Ocean)
- 3) Develop better skills for seasonal prediction to satisfy societal needs
- 4) Paleo-climate studies (perennial IOD in the early Pliocene warm period ?)

**All Tokyo/Yokohama activities
on IOD
are found at the following
IOD home page**

**[http://www.jamstec.go.jp/
frcgc/research/p1/iod/](http://www.jamstec.go.jp/frcgc/research/p1/iod/)**

TOPEX/POSEIDON, ERS1/2

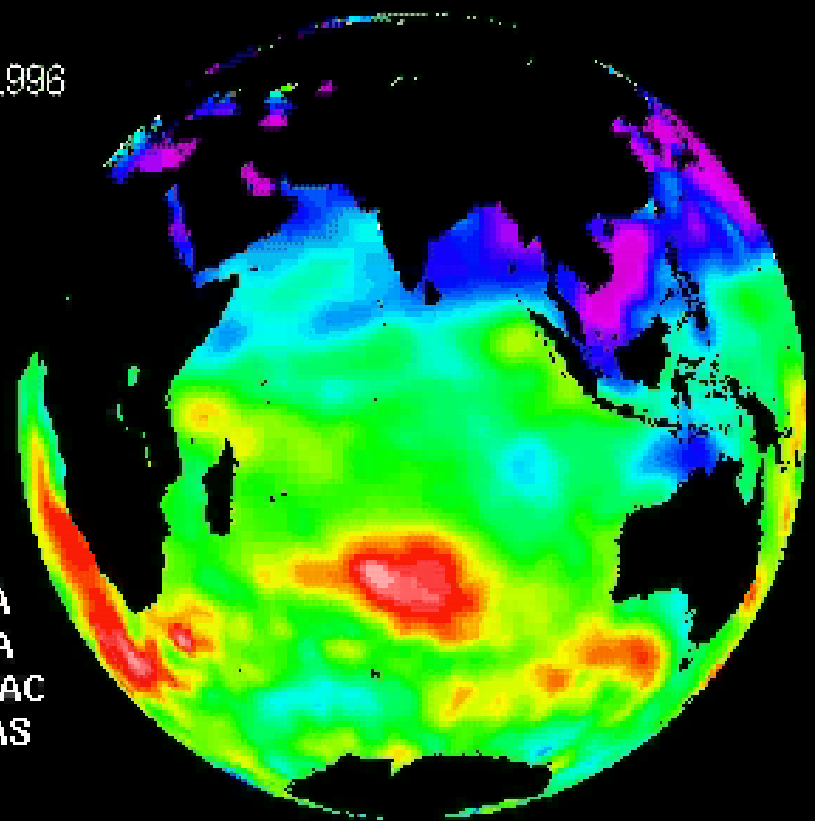


-18 -2 14

sea level anomaly (cm)

01 Jan 1996

AVHRR PATHFINDER

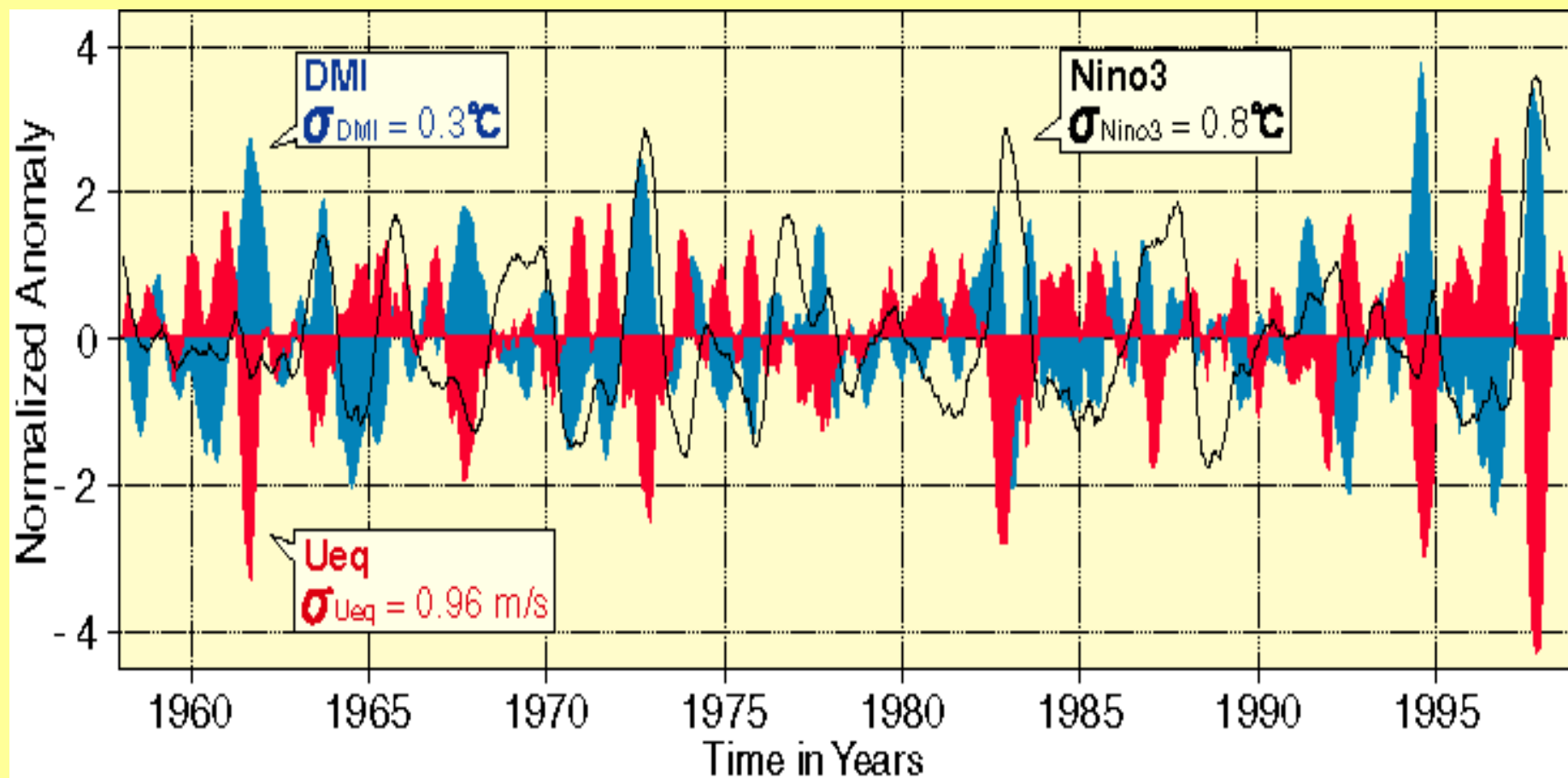


-2.5 0 2.5

sst anomaly (degrees C)

NASA
NOAA
PO.DAAC
RSMAS

Dipole Mode Index

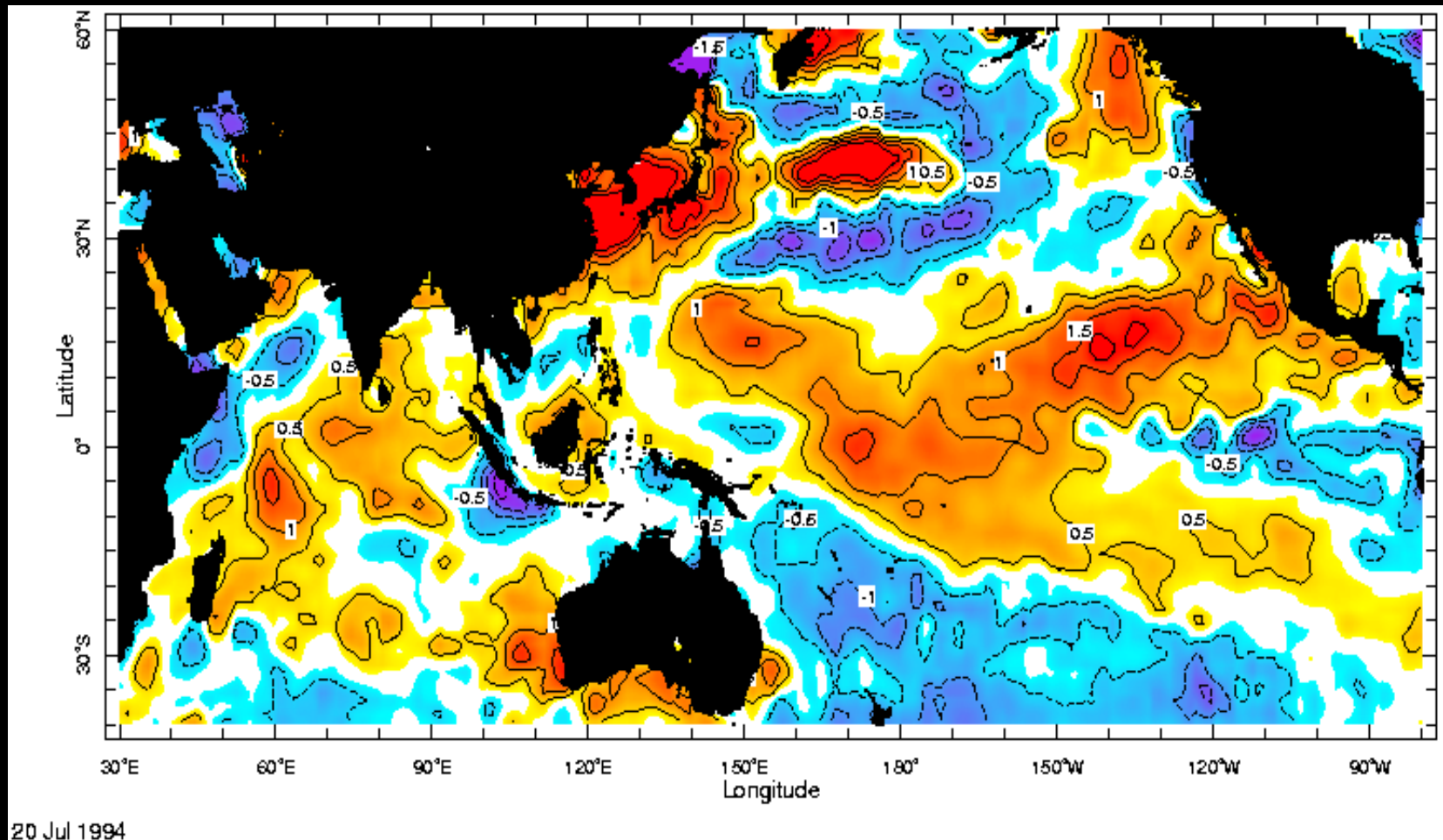


The Dipole Mode Index (DMI) was introduced by Saji et al. (1999) as the SST difference between the western tropical Indian Ocean ($50^{\circ}\text{E} - 70^{\circ}\text{E}$, $10^{\circ}\text{S} - 10^{\circ}\text{N}$) and the eastern tropical Indian Ocean ($90^{\circ}\text{E} - 110^{\circ}\text{E}$, $10^{\circ}\text{S} - \text{Equator}$).

The 501 months out of 1548 months from 1871 through 1999 correspond to the dipole month (based on GISST data). Out of these 501 months, the index is significant above one sigma for 167 months. The 48 months out of the 167 IOD months correspond to ENSO months. This means that the DMI Index and the ENSO index are not orthogonal each other in a statistical sense.

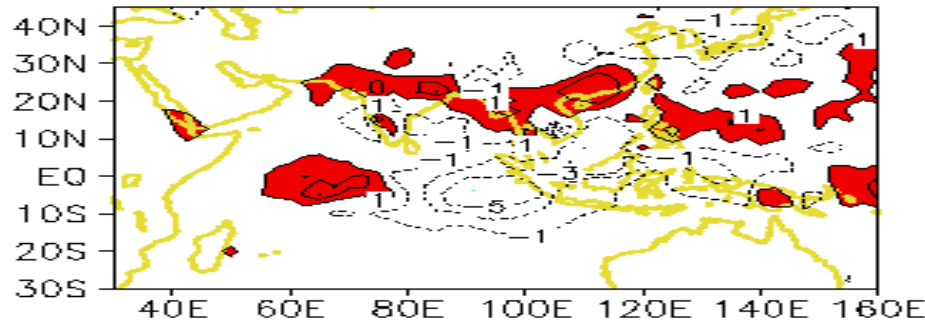
SST Anomaly in July 1994

We had extremely hot summer in East Asia.

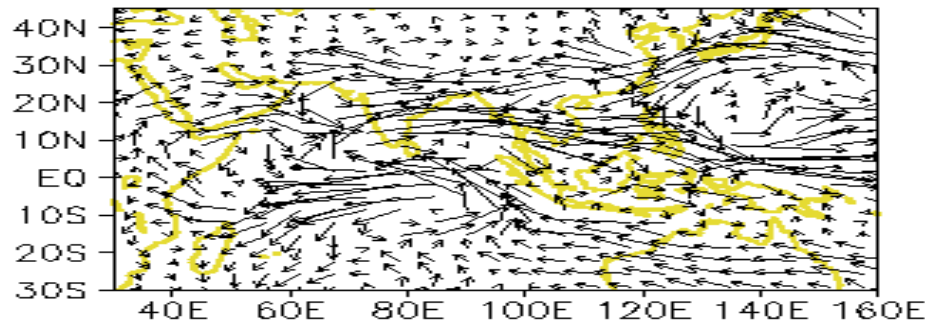


Rain and Moisture Transport Anomalies during Summer Months in 1994

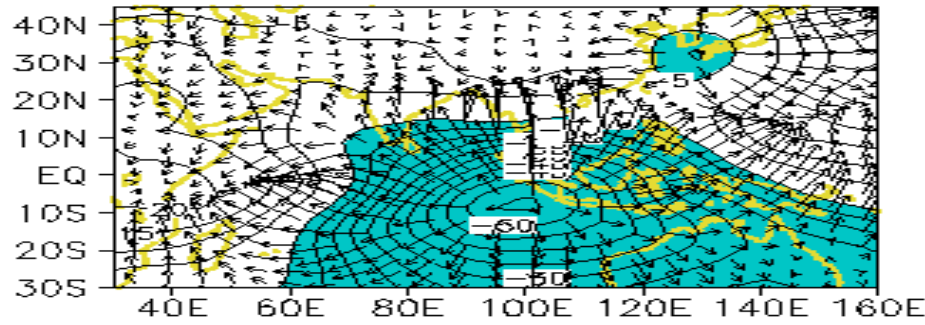
JJAS Rain Anom (mm/day)



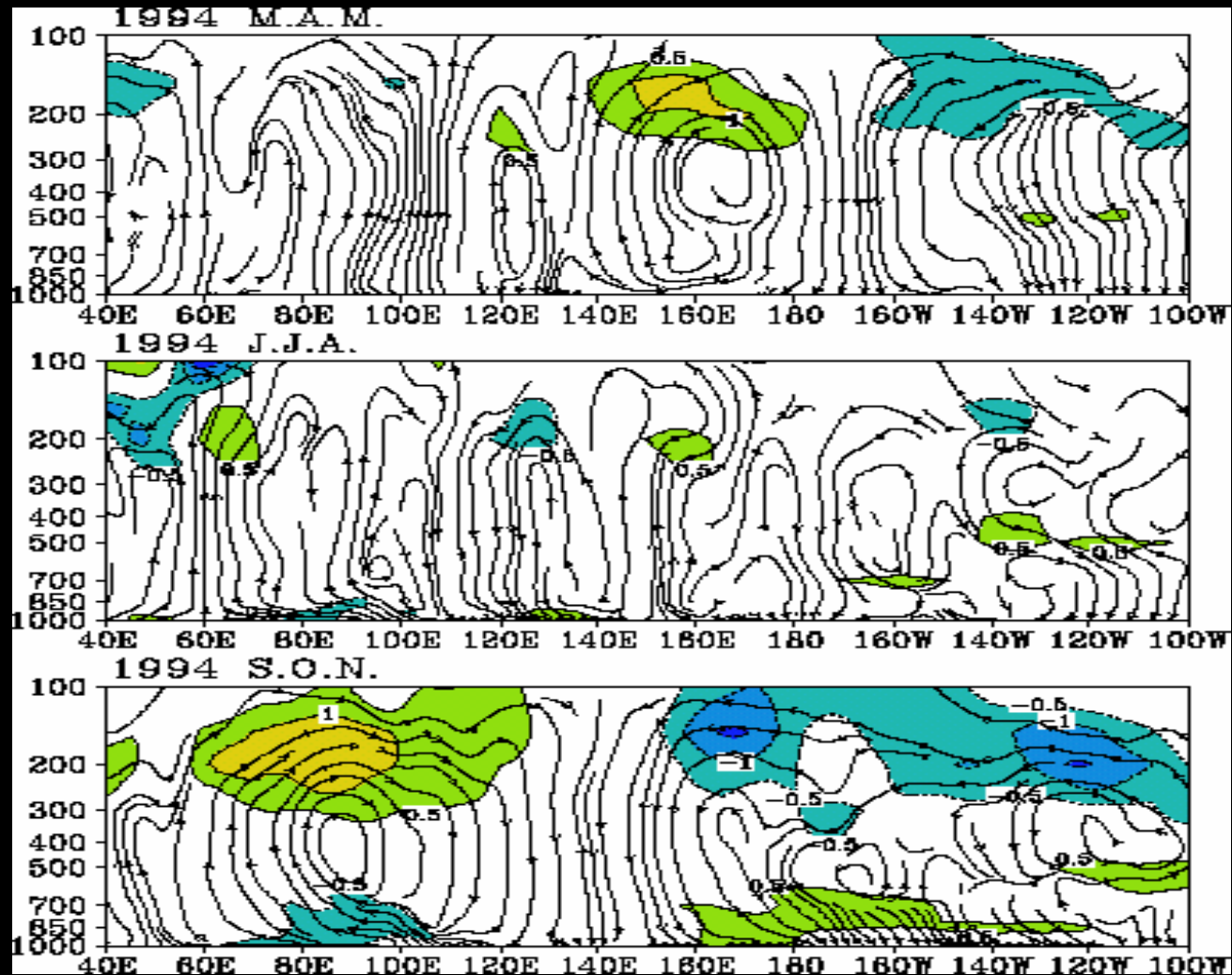
JJAS ROT Q Anom \longrightarrow 75 kg m⁻¹ s⁻¹



JJAS DIV Q Anom \longrightarrow 25 kg m⁻¹ s⁻¹



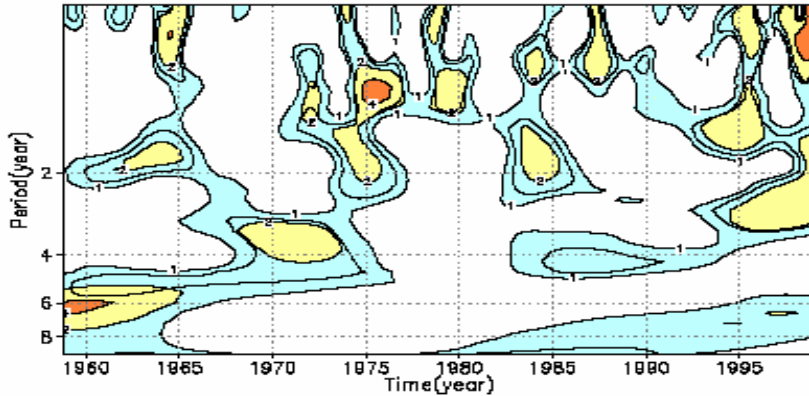
Anomalous Walker Circulation during Summer Months in 1994



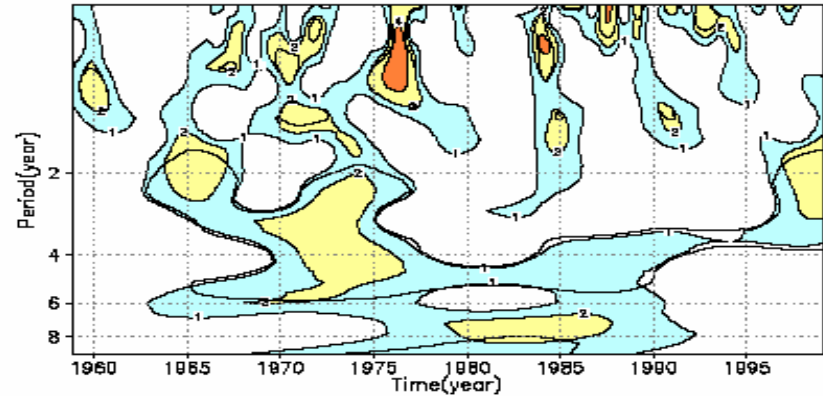
Zonal dipolar oscillation

Linkage between the eastern pole and the western pole is revealed by removing the ENSO influence.

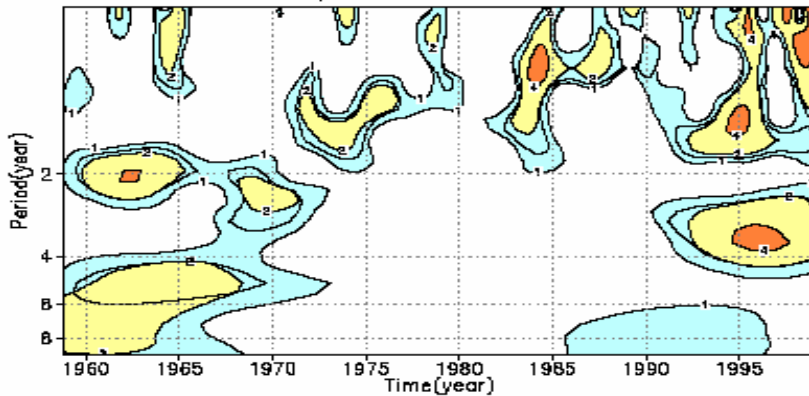
Wavelet spectrum of EAST IO



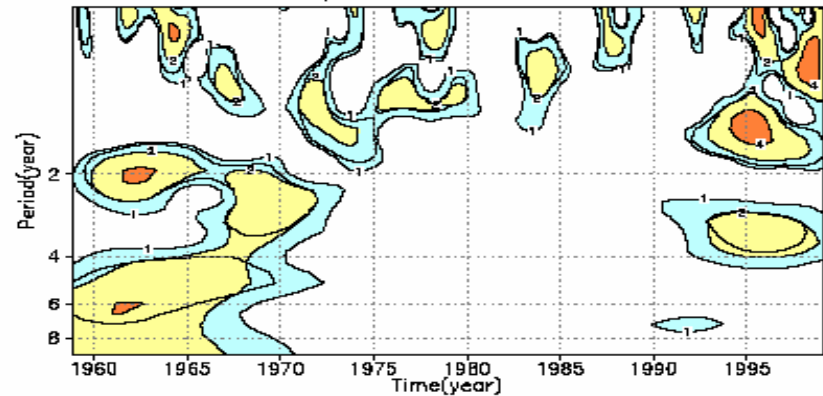
Wavelet spectrum of WEST IO



Wavelet spectrum of EAST IO-ENSO



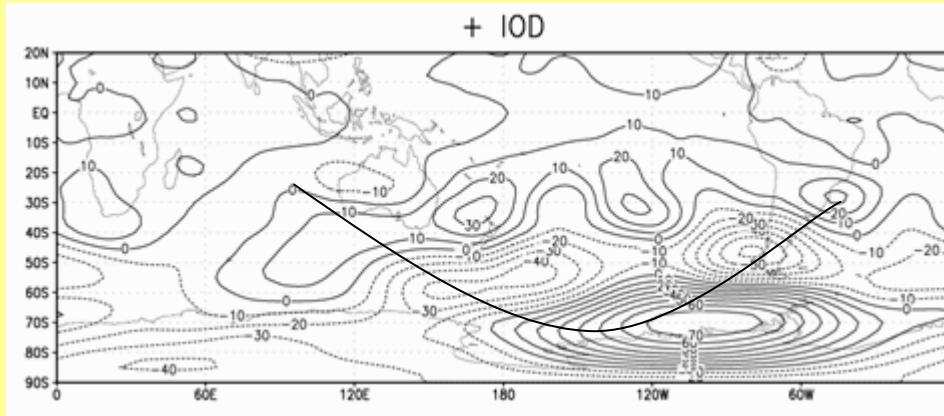
Wavelet spectrum of WEST IO-ENSO



IOD Teleconnection in the Southern Hemisphere:

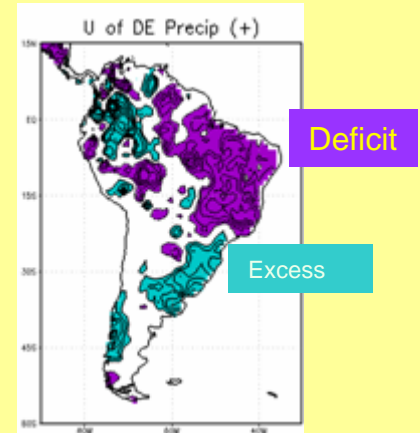
Impact on La Plata Rainfall

Pure Positive IOD Composite of 200 hPa Geopotential Height Anomalies (Oct-Nov)



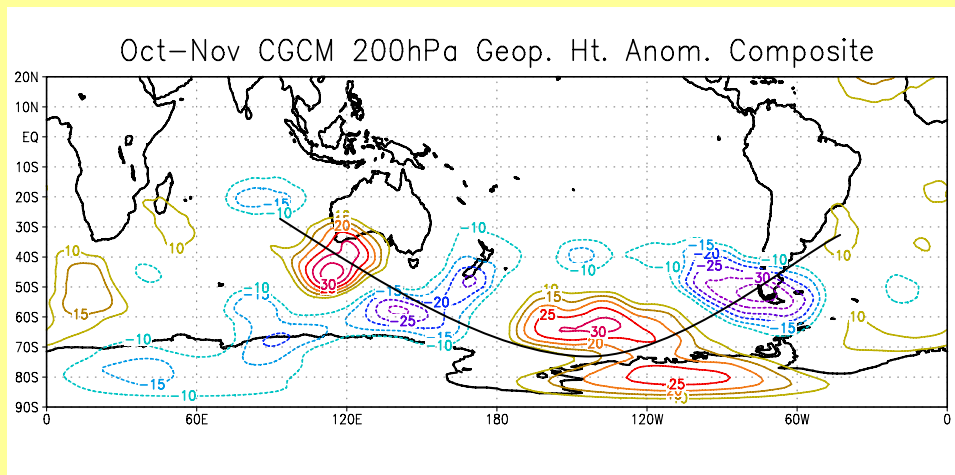
NCEP/NCAR
Reanalysis

Observed
Gridded
data

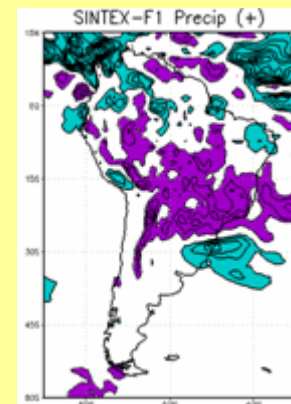


Deficit

Excess



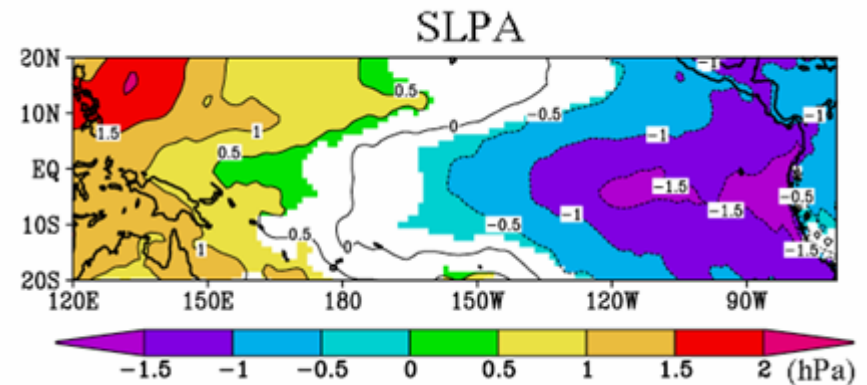
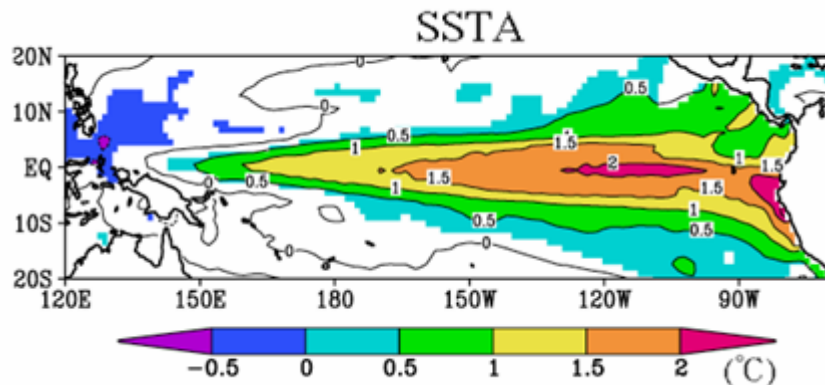
SINTEX-F



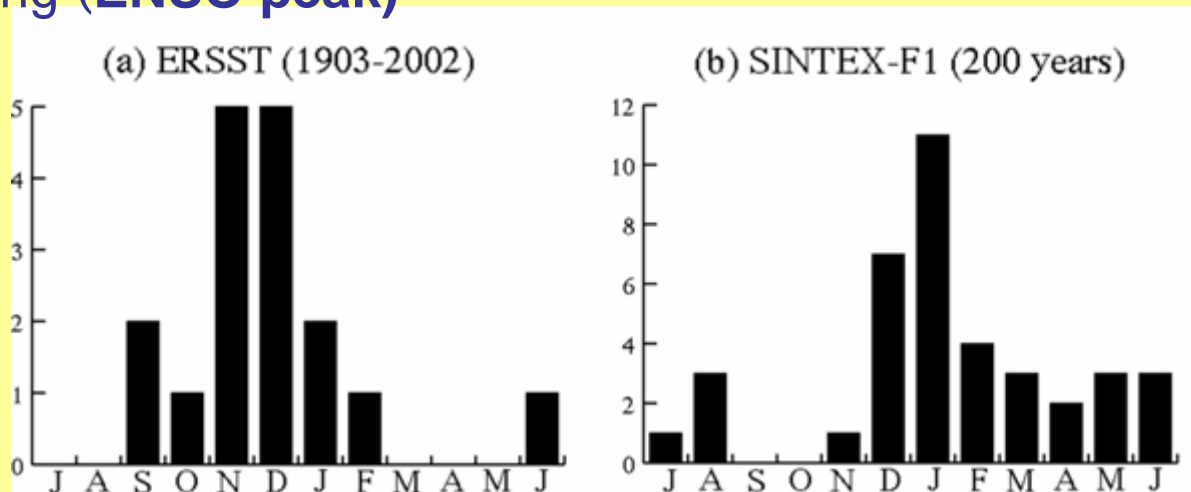
Simulated El Niño

El Niño composite: Dec.(0)

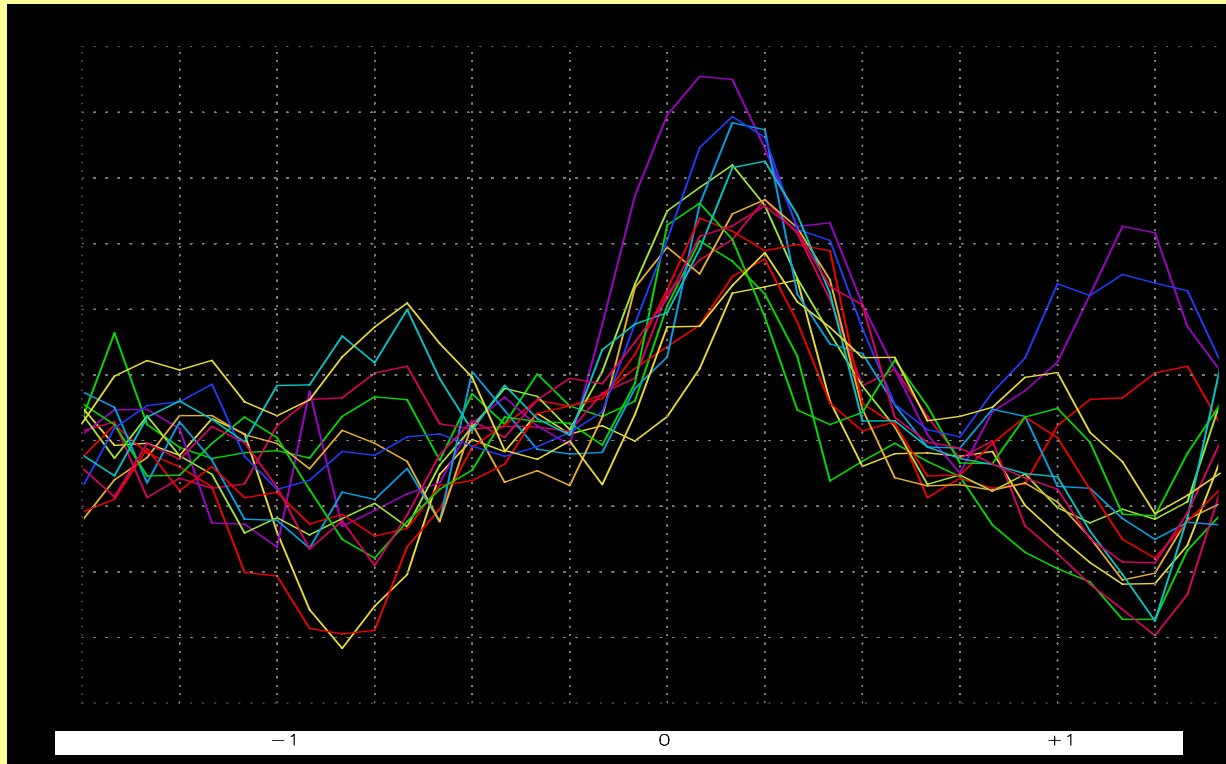
(color : significant at 95%)



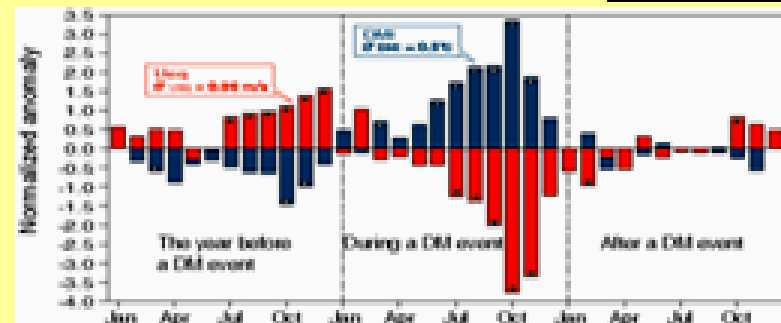
Phase locking (ENSO peak)



Capturing the Seasonal Phase Locking Character of the IOD



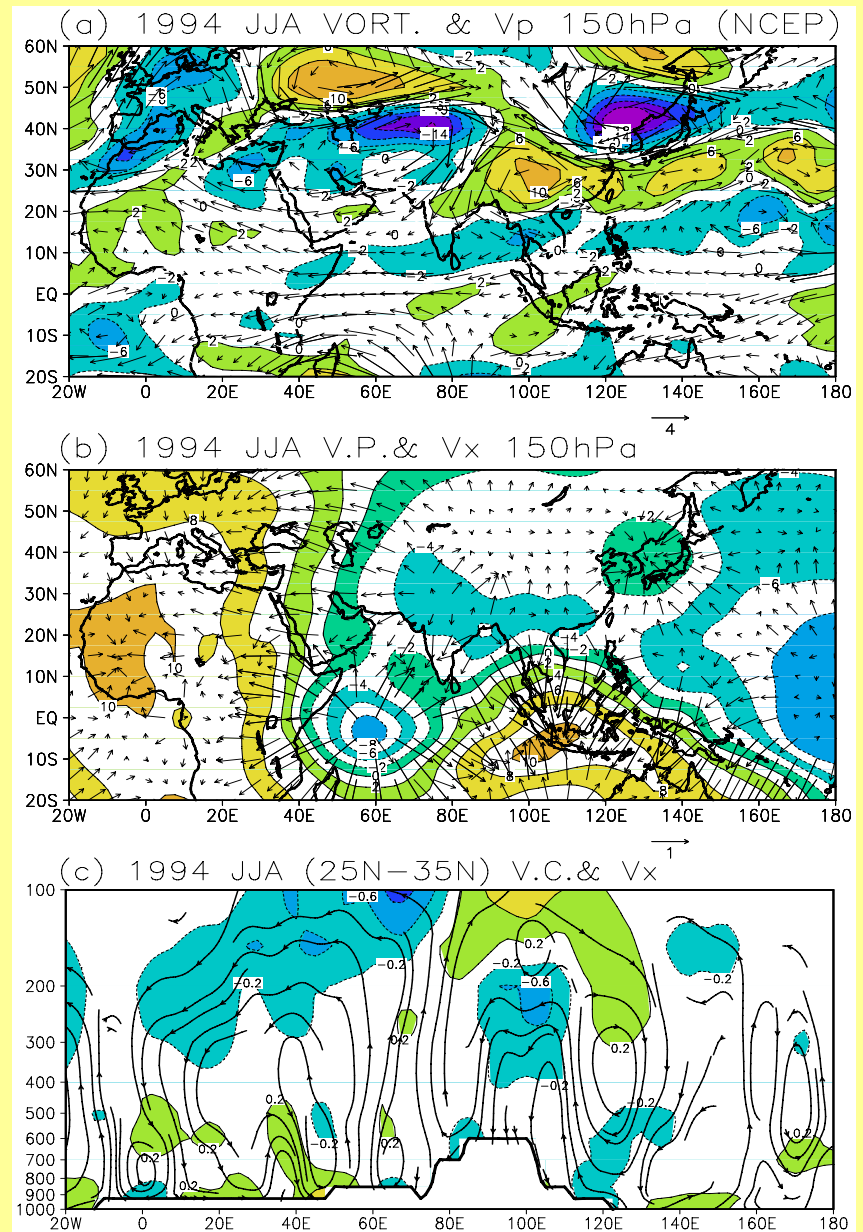
Observed –
Saji et al. 1999



(a) JJA mean anomalous vorticity (to be multiplied by $1 \times 10^{-6} \text{ s}^{-1}$) along with the rotational wind ($\text{m} \cdot \text{s}^{-1}$) at 150hPa in 1994.

(b) JJA mean velocity potential along with the divergent wind ($\text{m} \cdot \text{s}^{-1}$) at 150hPa in 1994. The contour interval is $4 \times 10^{-5} \text{ m}^2 \cdot \text{s}^{-1}$.

(c) JJA mean zonal-vertical circulation averaged over ($25^\circ\text{N}-35^\circ\text{N}$). The contours denote the zonal component of the divergent wind with contour interval of $0.2 \text{ m} \cdot \text{s}^{-1}$



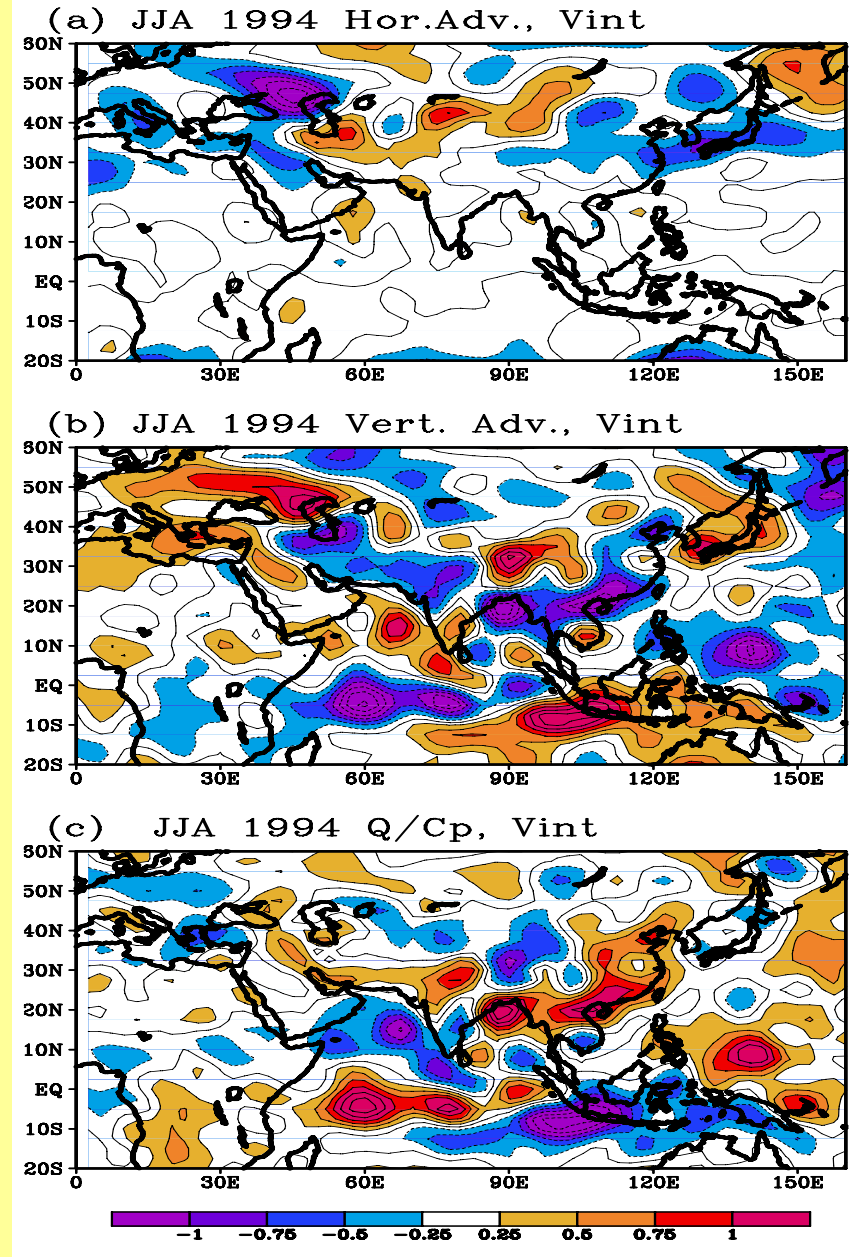
JJA mean vertically integrated thermal balance in 1994.

(Upper) The anomalous horizontal advection of temperature,

(Middle) The anomalous vertical advection of potential temperature, and

(Lower) The anomalous diabatic heating rate.

All these quantities are vertically averaged over pressure from surface to 100hPa. The unit is $^{\circ}\text{C}\cdot\text{d}^{-1}$.

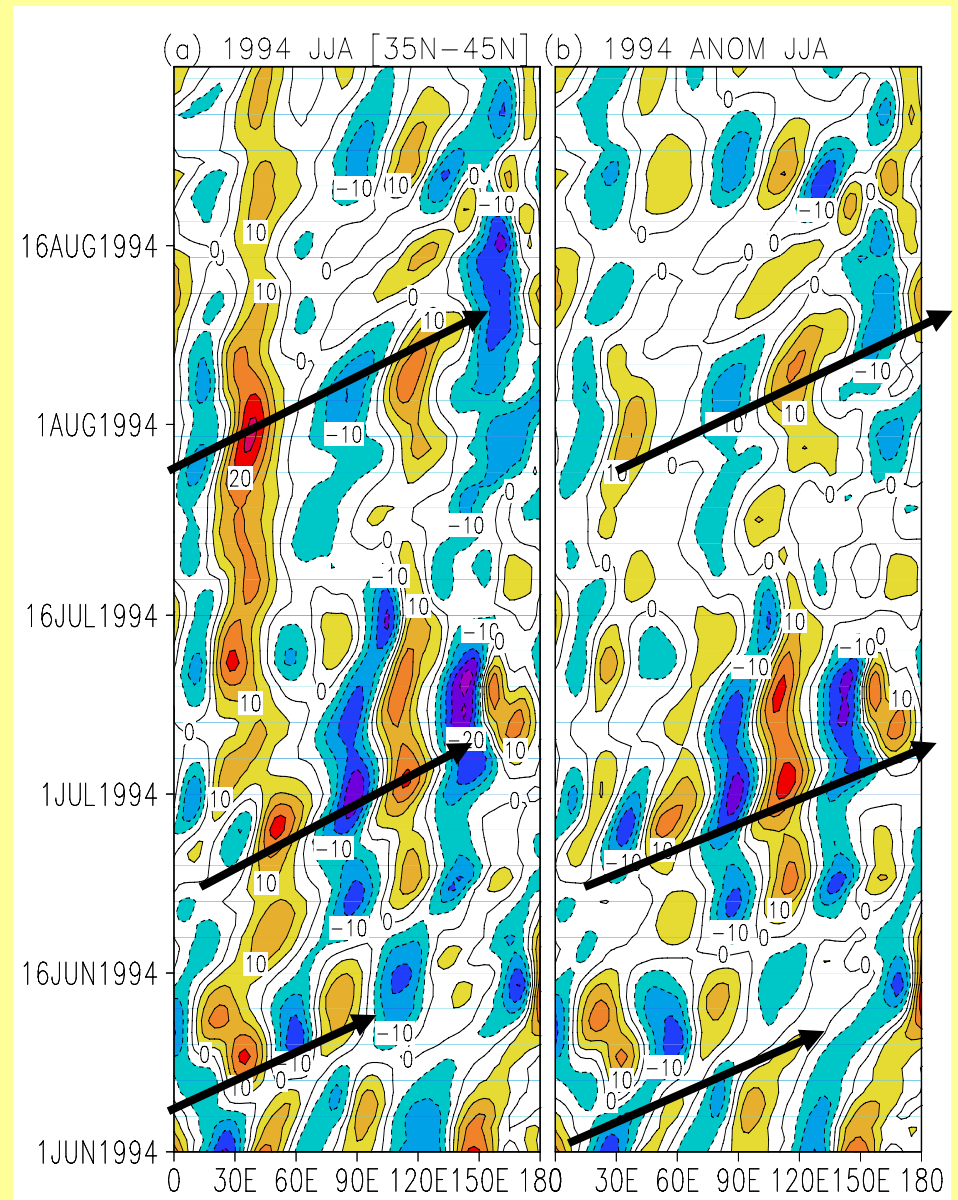


Rossby wave propagation

(a) X-t diagram for the meridional wind component averaged over [35N-45N] at 200hPa for 1994

(b) Anomalies in 1994.

Contour intervals are 5m/s. Time-series has been smoothed using a 5day running mean.



East African Short Rains:

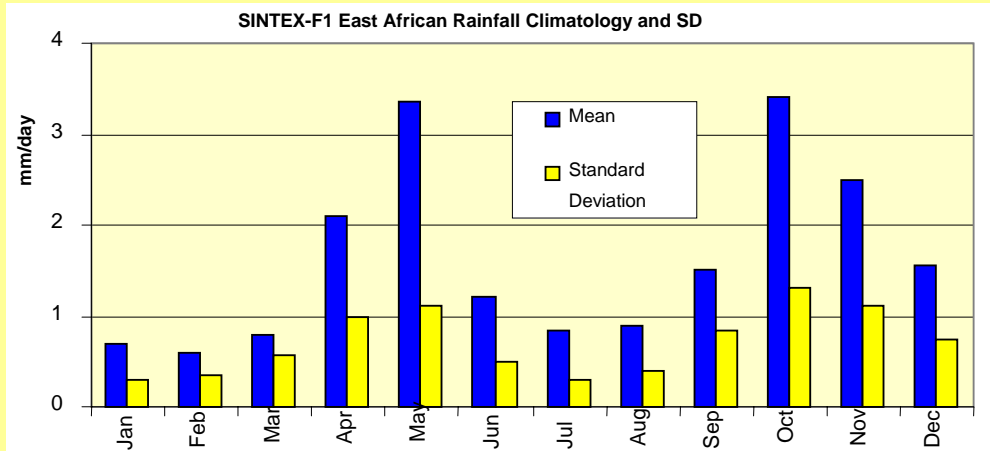
IOD Influence rather than ENSO influence

Non-orthogonality of both time series has misled climatologists for a long period.

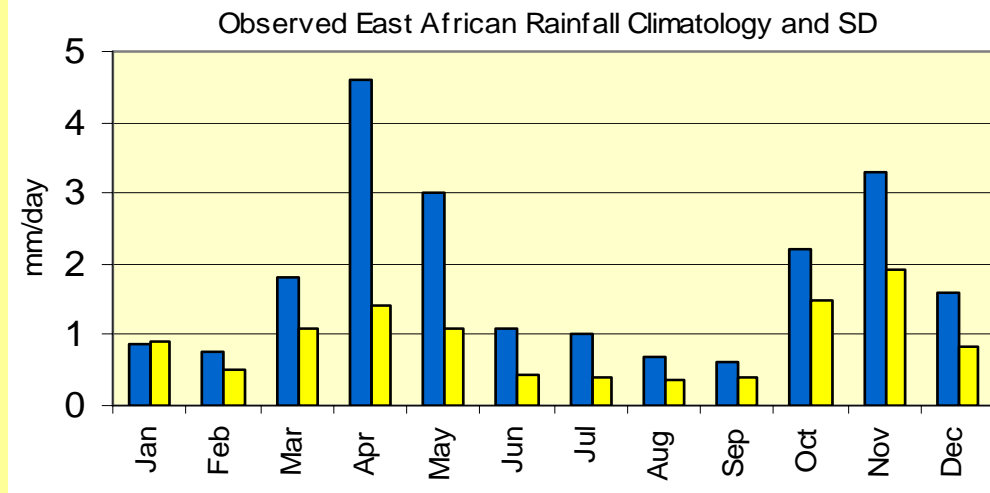
There was a danger of man-made disaster in local agriculture !!

East African Short Rains as simulated by SINTEX-F

MODEL
(200-yr data)



Obs.
(50-yr data)



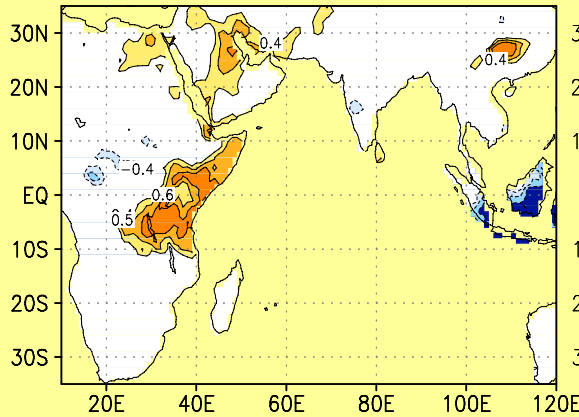
Climatology of the East African rainfall along with monthly standard deviations from SINTEX-F1 simulation results (upper panel) and observation (lower panel).



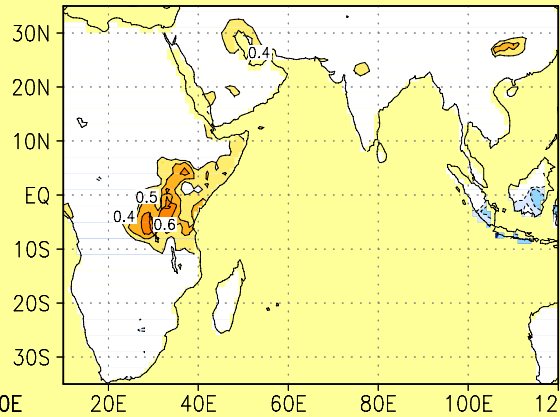
Observation

Correlation and Partial Correlation of SLP DMI and Rainfall from observed data

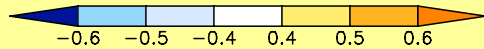
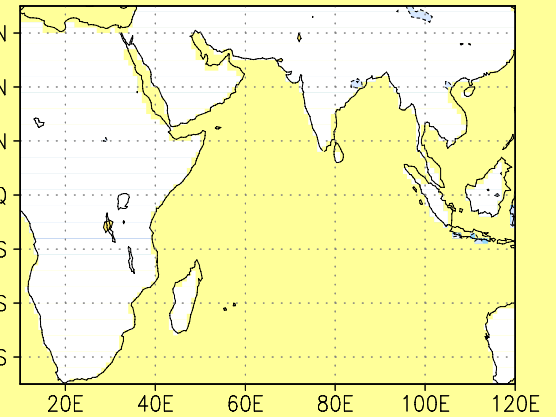
Corrl. SON SLPDMI Rainfall Data



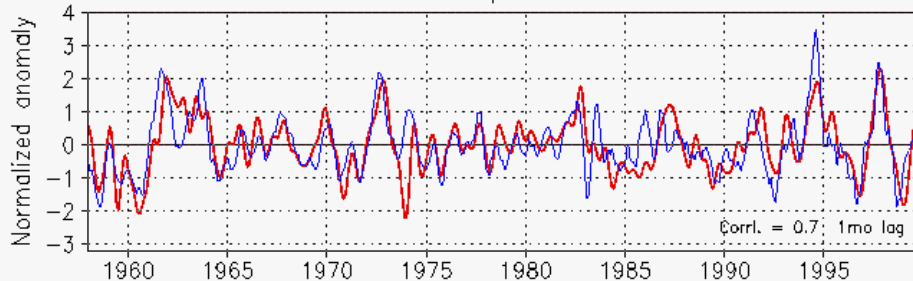
PCorrl. ENSO Removed



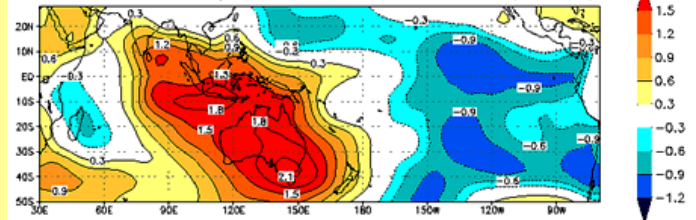
PCorrl. IOD Removed



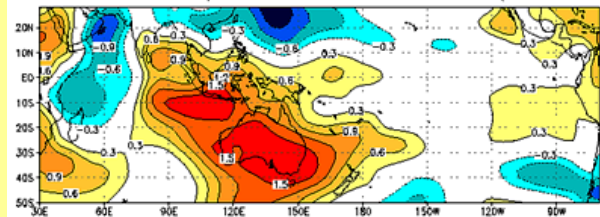
SST and SLP Dipole Mode Indices



Normalized Composite SLP Anm. Jun–Oct (All IOD)

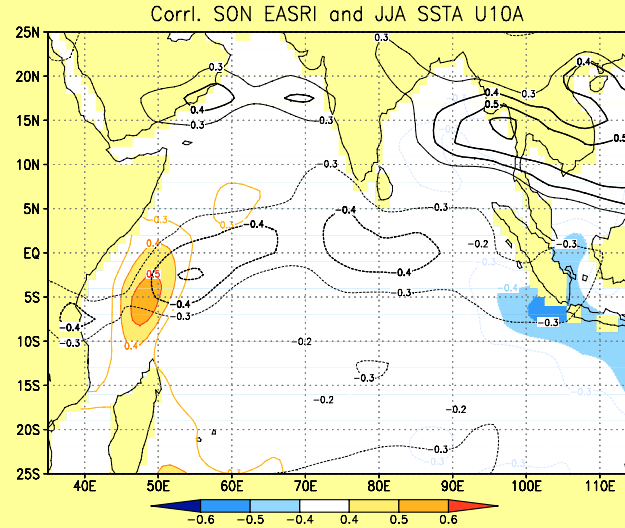
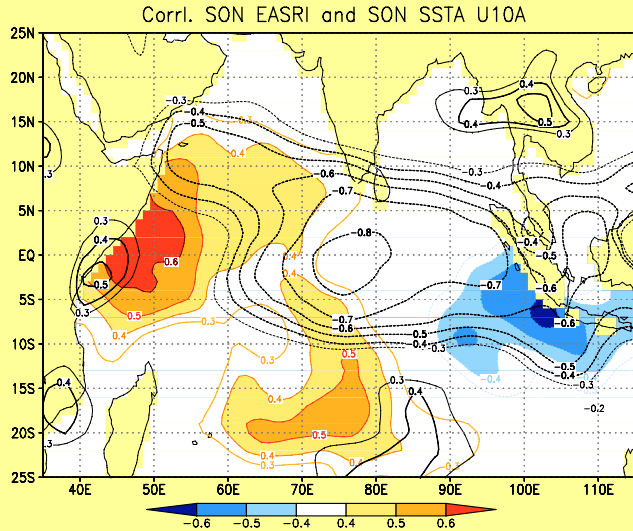


Normalized Composite SLP Anm. Jun–Oct (Pure IOD)



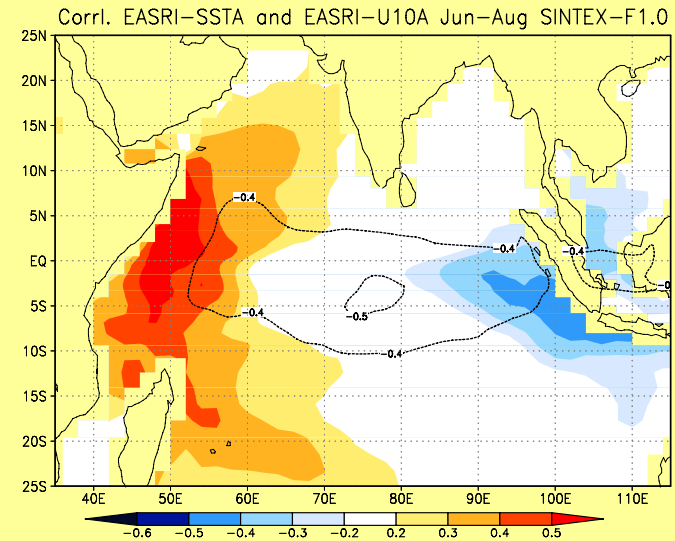
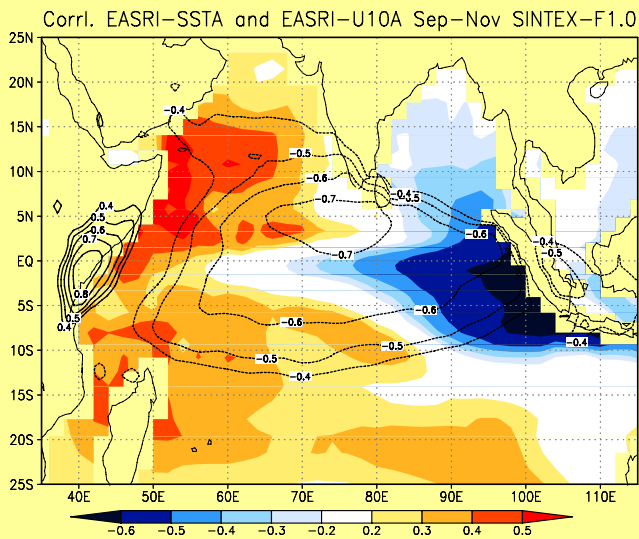
EASR Index Correlation with SSTA (shaded) and Zonal Wind Anomaly (contour)

Obs.



Observed

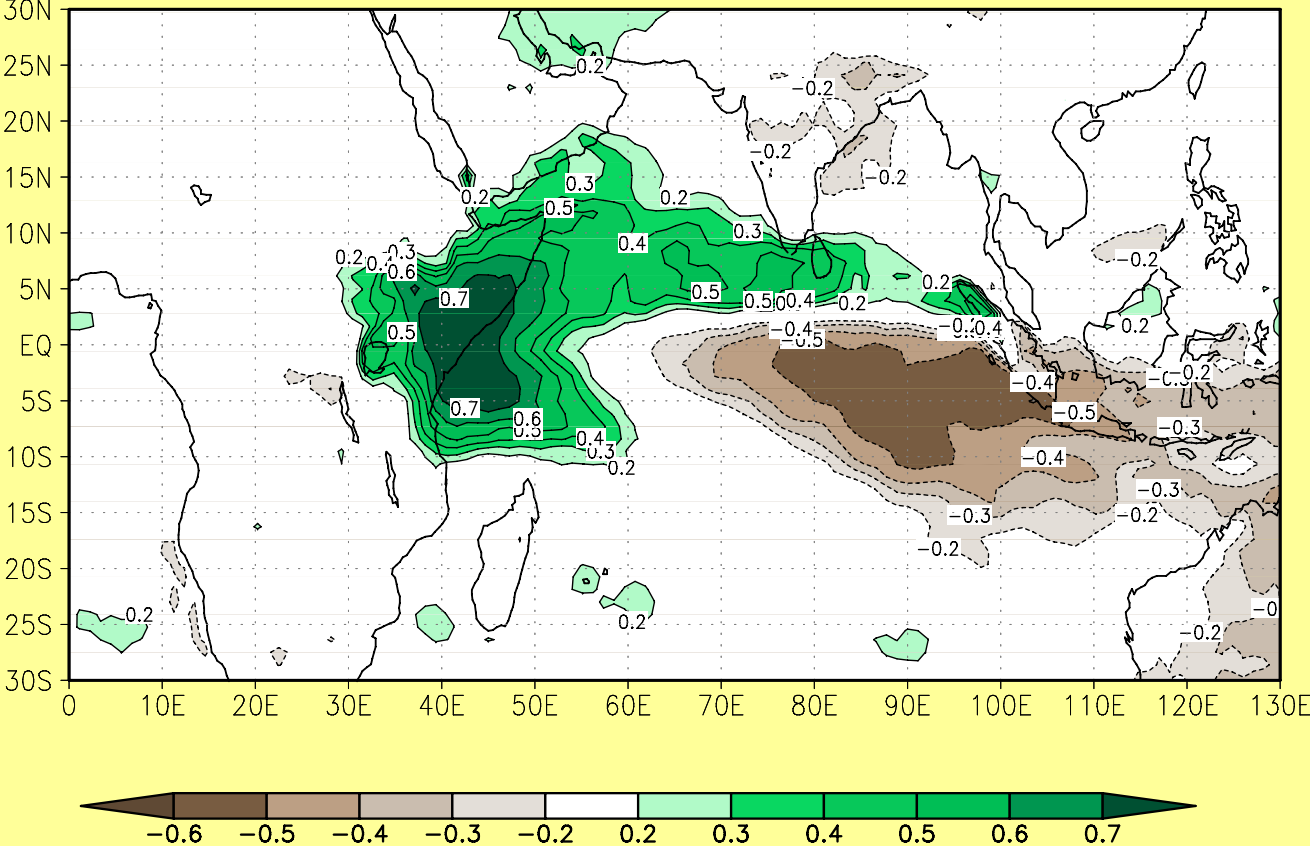
Model



SINTEX-F1

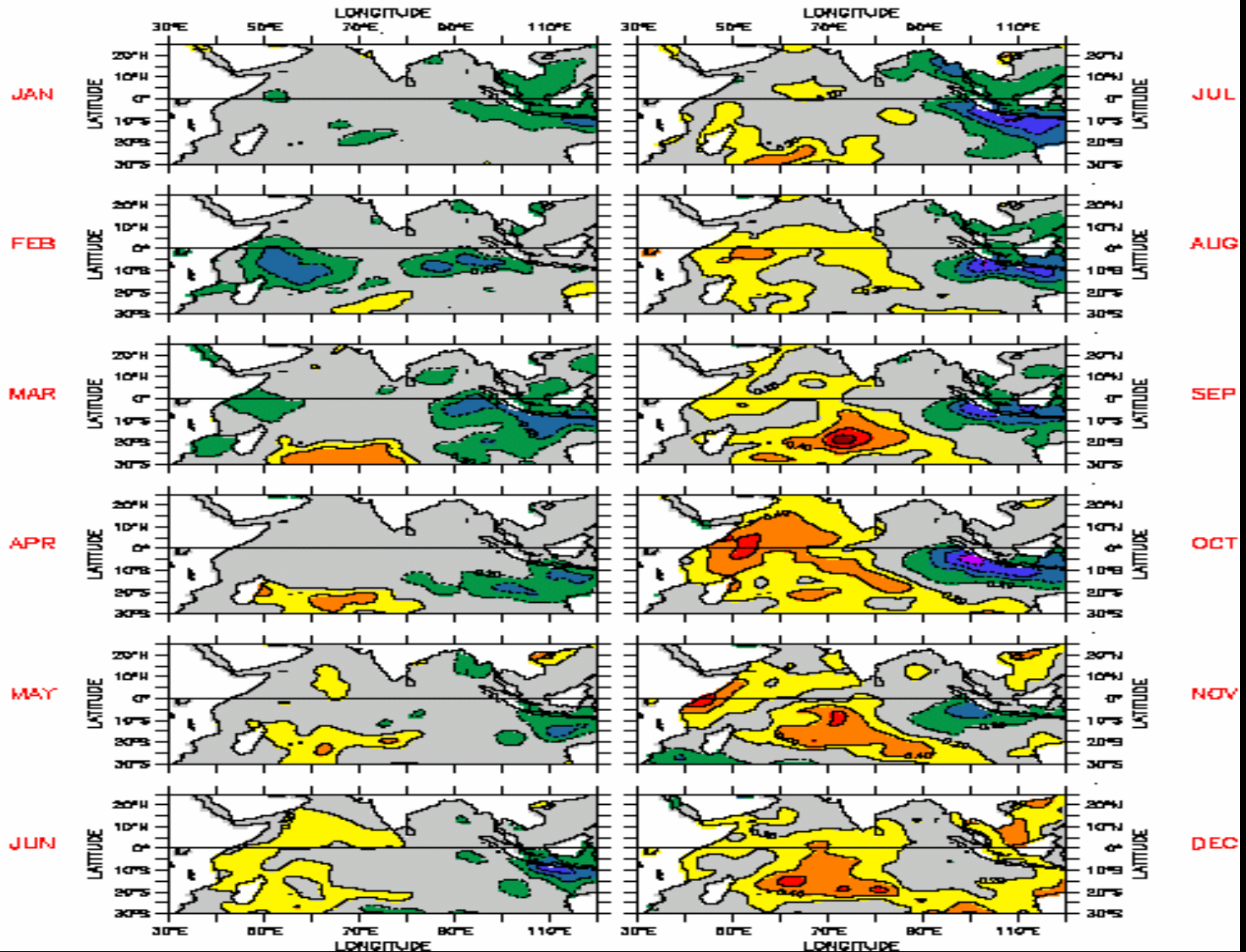
Correlation of the EASR index with the rainfall anomalies (SINTEX-F simulation results)

Corrl. SON EASRI and SON RA SINTEX-F1.0



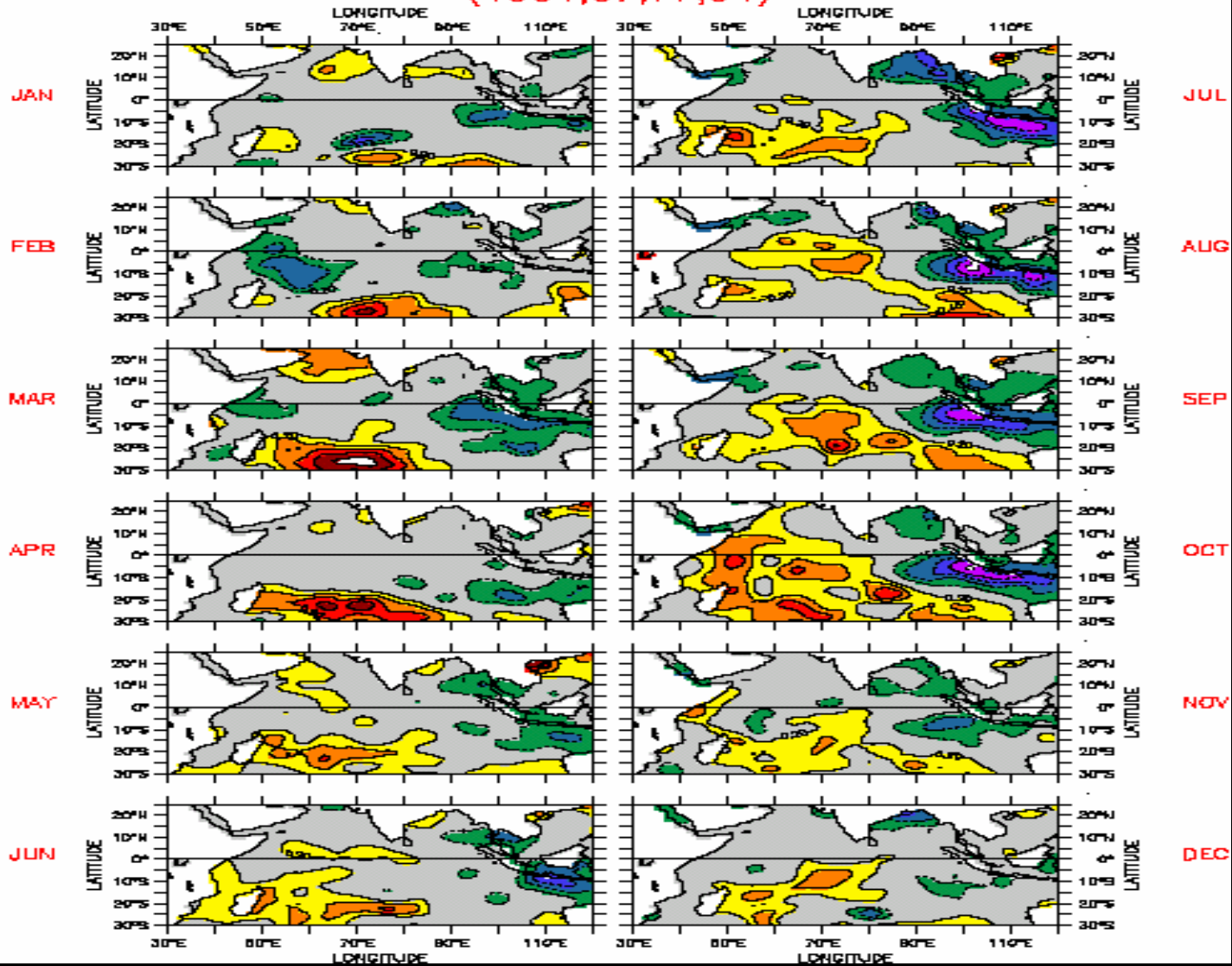
IOD Composites

IOD Composites (1961,67,72,77,82,94,97)



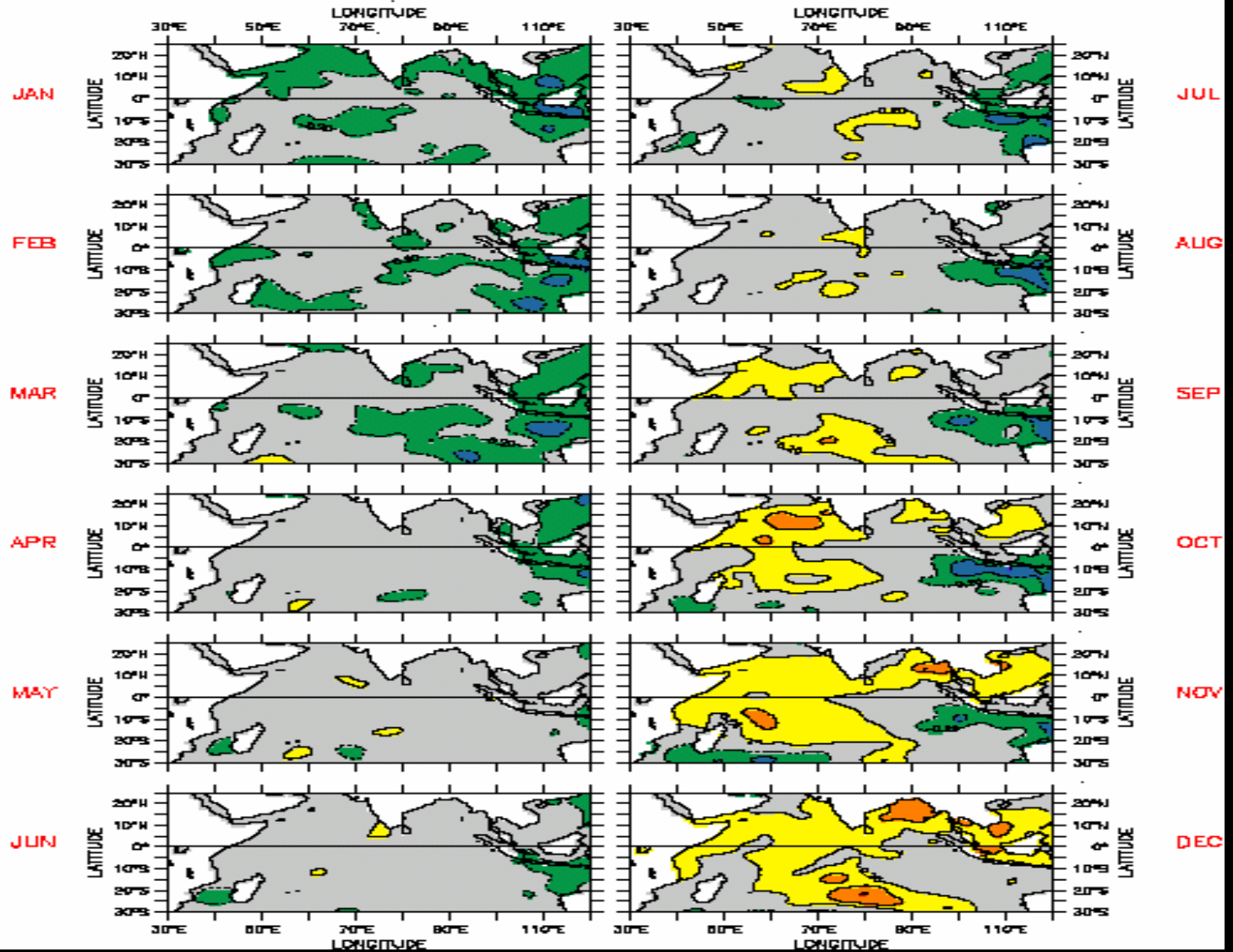
Pure IOD composites

Pure IOD composites
(1961,67,77,94)



ENSO Composites

ENSO Composites (1963,65,69,72,76,82,86,87,91,97)



Pure ENSO Composites

Pure ENSO composites
(1963,65,69,76,85,87,91)

